Chapter 2
Linear Perturbations in Galileon Gravity Models

[1]We discussed in the previous chapter that, before undergoing dedicated studies of nonlinear structure formation in modified gravity models, one should first learn about their goodness-of-fit to the data from the CMB, SNIa and BAO. In this chapter, we take the first steps towards using these data to constrain the Covariant Galileon gravity model [2, 3] by studying its linear perturbation theory predictions.

In the Galileon model, the deviations from GR are mediated by a scalar field φ, dubbed the Galileon, whose Lagrangian density is invariant under the Galilean shift symmetry $\partial_\mu\varphi \to \partial_\mu\varphi + b_\mu$ (where b_μ is a constant vector), in flat spacetime. Such a field appears, for instance, as a brane-bending mode in the decoupling limit of the four-dimensional boundary effective action of the DGP braneworld model [4–6] which was proposed before the Galileon model. However, despite being theoretically appealing, the self-accelerating branch of the DGP model is plagued by the ghost problems (energy states unbounded from below) [7–10]. Taking the decoupling limit of the DGP model as inspiration, it was shown in Ref. [2] that in four-dimensional Minkowski space there are only five Galilean invariant Lagrangians that lead to second-order field equations, despite containing highly nonlinear derivative self-couplings of the scalar field. The second-order nature of the equations of motion is crucial to avoid the presence of Ostrogradski ghosts [11]. Furthermore, the structure of these five Lagrangians is such that their classical solutions receive no quantum corrections to any loop order in perturbation field theory [12], i.e., the theory is *non-renormalizable*. This means that the theory is an effective field theory whose classical solutions can be trusted up to the energy scale above which a quantum completion of the theory becomes inevitable. In Ref. [3, 13], it was shown how these Lagrangians could be generalised to curved spacetimes. These authors concluded that explicit couplings between the Galileon field derivatives and curvature tensors are needed to keep the equations of motion up to second-order (see Ref. [14] for a recent discussion about how such couplings are not strictly needed). Such couplings however break the

[1]The content in this chapter is based on the article Barreira et al. "Linear perturbations in Galileon gravity models", Phys. Rev. D 86, 124016, Published 5 December 2012, http://dx.doi.org/10.1103/PhysRevD.86.124016 (Ref. [1]).

© Springer International Publishing Switzerland 2016

A. Barreira, *Structure Formation in Modified Gravity Cosmologies*,
Springer Theses, DOI 10.1007/978-3-319-33696-1_2

Galilean shift symmetry which is only a symmetry of the model in the limit of flat spacetime. The couplings of the Galileon field to the curvature tensors and to itself in the equations of motion change the way in which particle geodesics responds to the matter distribution, which is why the Galileon model falls under the category of modified gravity.

Since the equations of motion are kept up to second order, it means that the Galileon model is a subclass of the more general Horndeski theory [15–17]. The Horndeski action is the most general single scalar field action one can write that yields only second order field equations of motion of the metric and scalar fields. Besides the Galileon model, it therefore encompasses simpler cases such as Quintessence (cf. Eq. (1.9)) and $f(R)$ (cf. Eq. (1.11)) models as well as other models which also involve derivative couplings of the scalar field that have recently generated some interest such as Kinetic Gravity Braiding [18–20], Fab-Four [21–25], K-mouflage (cf. Eq. (1.14)) and others [26–28]. An important difference between the Galileon model studied here and some other corners of Horndeski's general theory is that in the Galileon model there are no free functions.

In this chapter, we start by presenting the action and field equations of the Covariant Galileon model. We then derive the fully covariant and gauge invariant linearly perturbed field equations and solve them with a modified version of the `CAMB` code. We analyse the model predictions for the CMB temperature, CMB lensing and linear matter power spectra, and also for the time evolution of the lensing potential. We do this for a limited number of parameter values to illustrate how the model predictions are obtained. A main goal of this chapter is to build some intuition for the contraint results of Chap. 3.

2.1 The Covariant Galileon Model

The action of the covariant uncoupled Galileon model is given by [3]

$$S = \int d^4x\sqrt{-g}\left[\frac{\mathcal{R}}{16\pi G} - \frac{1}{2}\sum_{i=1}^{5} c_i\mathcal{L}_i - \mathcal{L}_m\right], \tag{2.1}$$

with

$$\begin{aligned}
\mathcal{L}_1 &= M^3\varphi,\\
\mathcal{L}_2 &= \nabla_\mu\varphi\nabla^\mu\varphi,\\
\mathcal{L}_3 &= \frac{2}{M^3}\Box\varphi\nabla_\mu\varphi\nabla^\mu\varphi,\\
\mathcal{L}_4 &= \frac{1}{M^6}\nabla_\mu\varphi\nabla^\mu\varphi\left[2(\Box\varphi)^2 - 2(\nabla_\mu\nabla_\nu\varphi)(\nabla^\mu\nabla^\nu\varphi)\right.\\
&\quad \left.-R\nabla_\mu\varphi\nabla^\mu\varphi/2\right],
\end{aligned}$$

$$\mathcal{L}_5 = \frac{1}{M^9}\nabla_\mu\varphi\nabla^\mu\varphi\left[(\Box\varphi)^3 - 3(\Box\varphi)(\nabla_\mu\nabla_\nu\varphi)(\nabla^\mu\nabla^\nu\varphi)\right.$$
$$+2(\nabla_\mu\nabla^\nu\varphi)(\nabla_\nu\nabla^\rho\varphi)(\nabla_\rho\nabla^\mu\varphi)$$
$$\left.-6(\nabla_\mu\varphi)(\nabla^\mu\nabla^\nu\varphi)(\nabla^\rho\varphi)G_{\nu\rho}\right], \tag{2.2}$$

where $\mathcal{R}$ is the Ricci curvature scalar, g is the determinant of the metric $g_{\mu\nu}$, and $M^3 \equiv M_{\rm Pl}H_0^2$ with H_0 being the present-day Hubble expansion rate. The five terms in the Lagrangian density are fixed by the Galilean invariance in a flat spacetime, $\partial_\mu\varphi \to \partial_\mu\varphi + b_\mu$, and c_{1-5} are dimensionless constants. The explicit couplings to the Ricci scalar $\mathcal{R}$ and the Einstein tensor $G_{\mu\nu}$ in $\mathcal{L}_4$ and $\mathcal{L}_5$ break the Galilean symmetry, but are necessary to limit the equations of motion to second-order in field derivatives (and hence free from Ostrogradski ghosts) in spacetimes such as FRW [3].[2] We set the potential term to zero ($c_1 = 0$), as we are only interested in cases where cosmic acceleration is driven by the kinetic terms of the field. Before proceeding, we note in passing that $\mathcal{L}_4$ and $\mathcal{L}_5$ are associated with some theoretical problems related to the smallness of the energy cutoff below which the theory is valid, as discussed in [2, 29]. In general, in this thesis, we shall always be more concerned about the observational consequences of the models, although such theoretical problems should always be kept in mind.

Besides the terms which appear in the Galileon Lagrangians, $\mathcal{L}_i$, we also consider here a derivative coupling of the form $\mathcal{L}_{coupling} \sim G^{\mu\nu}\nabla_\mu\varphi\nabla_\nu\varphi$, which does not spoil the second-order nature of the equations [30–36]. Here, for comparison purposes, we follow [30] and add to Eq. (2.1) the Lagrangian density

$$\mathcal{L}_G = -c_G\frac{M_{\rm Pl}}{M^3}G^{\mu\nu}\nabla_\mu\varphi\nabla_\nu\varphi, \tag{2.3}$$

where c_G is a dimensionless constant. The phenomenology of $\mathcal{L}_G$ is only studied in the present chapter, and not anywhere else in this thesis.

The modified Einstein field equations and the Galileon field equation of motion can be obtained by varying the action with respect to $g_{\mu\nu}$ and φ, respectively. Our derivation agrees with those present in the literature [3, 30] although we explicitly write the Riemann tensor in terms of the Ricci and Weyl tensors, whenever it leads to the cancellation of some terms and hence to a slight simplification of the final expressions. The Einstein field equations are given by:

$$G_{\mu\nu} = \kappa\left[T^f_{\mu\nu} + T^{c_2}_{\mu\nu} + T^{c_3}_{\mu\nu} + T^{c_4}_{\mu\nu} + T^{c_5}_{\mu\nu} + T^{c_G}_{\mu\nu}\right], \tag{2.4}$$

[2] These curvature couplings act as counter terms that cancel the higher derivative terms that arise from the naive promotion of the partial derivatives to covariant ones. However, Ref. [14] has shown that, due to hidden constraints, these curvature couplings are indeed not stricly necessary.

where

$$T^{c_2}_{\mu\nu} = c_2\left[\nabla_\mu\varphi\nabla_\nu\varphi - \frac{1}{2}g_{\mu\nu}\nabla^\alpha\varphi\nabla_\alpha\varphi\right], \tag{2.5}$$

$$T^{c_3}_{\mu\nu} = \frac{c_3}{M^3}\left[2\nabla_\mu\varphi\nabla_\nu\varphi\Box\varphi + 2g_{\mu\nu}\nabla_\alpha\varphi\nabla_\beta\varphi\nabla^\alpha\nabla^\beta\varphi - 4\nabla^\lambda\varphi\nabla_{(\mu}\varphi\nabla_{\nu)}\nabla_\lambda\varphi\right], \tag{2.6}$$

$$\begin{aligned}T^{c_4}_{\mu\nu} = {}& \frac{c_4}{M^6}g_{\mu\nu}\Big[(\Box\varphi)^2\nabla_\lambda\varphi\nabla^\lambda\varphi - \frac{1}{12}R\left(\nabla_\alpha\varphi\nabla^\alpha\varphi\right)^2 + 4\Box\varphi\nabla^\alpha\varphi\nabla^\beta\varphi\nabla_\alpha\nabla_\beta\varphi \\ & - 4\nabla_\lambda\nabla_\alpha\varphi\nabla^\lambda\nabla_\beta\varphi\nabla^\alpha\varphi\nabla^\beta\varphi - \nabla_\lambda\varphi\nabla^\lambda\varphi\nabla_\alpha\nabla_\beta\varphi\nabla^\alpha\nabla^\beta\varphi - R_{\alpha\beta}\nabla^\alpha\varphi\nabla^\beta\varphi\nabla_\lambda\varphi\nabla^\lambda\varphi\Big] \\ & + \frac{c_4}{M^6}\Big[2(\Box\varphi)^2\nabla_\mu\varphi\nabla_\nu\varphi + 2\nabla_\lambda\varphi\nabla^\lambda\varphi\nabla^\rho\varphi R_{\rho(\mu}\nabla_{\nu)}\varphi - 8\Box\varphi\nabla^\lambda\varphi\nabla_\lambda\nabla_{(\mu}\varphi\nabla_{\nu)}\varphi \\ & - 2\nabla_\alpha\nabla_\beta\varphi\nabla^\alpha\nabla^\beta\varphi\nabla_\mu\varphi\nabla_\nu\varphi + 8\nabla^\lambda\varphi\nabla_\rho\nabla_\lambda\varphi\nabla^\rho\nabla_{(\mu}\varphi\nabla_{\nu)}\varphi - 2\Box\varphi\nabla_\lambda\varphi\nabla^\lambda\varphi\nabla_\mu\nabla_\nu\varphi \\ & - 4\nabla_\alpha\nabla_\beta\varphi\nabla^\alpha\varphi\nabla^\beta\varphi\nabla_\mu\nabla_\nu\varphi - \frac{2}{3}R\nabla_\lambda\varphi\nabla^\lambda\varphi\nabla_\mu\varphi\nabla_\nu\varphi + \frac{1}{2}R_{\mu\nu}\left(\nabla_\alpha\varphi\nabla^\alpha\varphi\right)^2 \\ & + 2\nabla_\mu\nabla_\alpha\varphi\nabla_\nu\nabla^\alpha\varphi\nabla_\lambda\varphi\nabla^\lambda\varphi + 4\nabla_\mu\nabla_\alpha\varphi\nabla_\nu\nabla_\beta\varphi\nabla^\alpha\varphi\nabla^\beta\varphi + 2\mathcal{W}_{\mu\alpha\nu\beta}\nabla^\alpha\varphi\nabla^\beta\varphi\nabla_\lambda\varphi\nabla^\lambda\varphi\Big],\end{aligned} \tag{2.7}$$

$$\begin{aligned}T^{c_5}_{\mu\nu} = {}& \frac{c_5}{M^9}g_{\mu\nu}\Big[(\Box\varphi)^3\nabla_\lambda\varphi\nabla^\lambda\varphi + 3(\Box\varphi)^2\nabla^\alpha\nabla^\beta\varphi\nabla_\alpha\varphi\nabla_\beta\varphi - 3\Box\varphi\nabla_\lambda\varphi\nabla^\lambda\varphi\nabla_\alpha\nabla_\beta\varphi\nabla^\alpha\nabla^\beta\varphi \\ & - 6\Box\varphi\nabla^\alpha\nabla^\beta\varphi\nabla_\alpha\nabla_\lambda\varphi\nabla_\beta\varphi\nabla^\lambda\varphi + 2\nabla_\lambda\varphi\nabla^\lambda\varphi\nabla_\alpha\nabla^\beta\varphi\nabla_\beta\nabla^\gamma\varphi\nabla_\gamma\nabla^\alpha\varphi \\ & - 3\nabla_\alpha\nabla_\beta\varphi\nabla^\alpha\nabla^\beta\varphi\nabla_\rho\nabla_\sigma\varphi\nabla^\rho\varphi\nabla^\sigma\varphi + 6\nabla_\alpha\nabla_\beta\varphi\nabla^\beta\nabla^\gamma\varphi\nabla_\gamma\nabla_\lambda\varphi\nabla^\alpha\varphi\nabla^\lambda\varphi - R\Box\varphi\left(\nabla_\lambda\varphi\nabla^\lambda\varphi\right)^2 \\ & + \frac{3}{2}R_{\alpha\beta}\nabla^\alpha\nabla^\beta\varphi\left(\nabla_\lambda\varphi\nabla^\lambda\varphi\right)^2 + 3\nabla_\lambda\varphi\nabla^\lambda\varphi\nabla^\alpha\varphi\nabla^\beta\varphi\nabla^\gamma\nabla^\sigma\varphi\mathcal{W}_{\alpha\gamma\beta\sigma}\Big] \\ & + \frac{c_5}{M^9}\Big[(\Box\varphi)^3\nabla_\mu\varphi\nabla_\nu\varphi - 3(\Box\varphi)^2\nabla_\lambda\varphi\nabla^\lambda\varphi\nabla_\mu\nabla_\nu\varphi - 6(\Box\varphi)^2\nabla^\lambda\varphi\nabla_\lambda\nabla_{(\mu}\varphi\nabla_{\nu)}\varphi + 6\Box\varphi\nabla_\lambda\varphi\nabla^\lambda\varphi\nabla_\mu\nabla_\alpha\varphi\nabla_\nu\nabla^\alpha\varphi \\ & - 6\Box\varphi\nabla_\alpha\nabla_\beta\varphi\nabla^\alpha\varphi\nabla^\beta\varphi\nabla_\mu\nabla_\nu\varphi - 3\Box\varphi\nabla_\alpha\nabla_\beta\varphi\nabla^\alpha\nabla^\beta\varphi\nabla_\mu\varphi\nabla_\nu\varphi + 6\Box\varphi\nabla^\alpha\varphi\nabla^\beta\varphi\nabla_\mu\nabla_\alpha\varphi\nabla_\nu\nabla_\beta\varphi \\ & + 12\Box\varphi\nabla_\alpha\varphi\nabla^\alpha\nabla^\beta\varphi\nabla_\beta\nabla_{(\mu}\varphi\nabla_{\nu)}\varphi + 3\nabla_\lambda\varphi\nabla^\lambda\varphi\nabla_\alpha\nabla_\beta\varphi\nabla^\alpha\nabla^\beta\varphi\nabla_\mu\nabla_\nu\varphi - 6\nabla_\lambda\varphi\nabla^\lambda\varphi\nabla^\alpha\nabla^\beta\varphi\nabla_\mu\nabla_\alpha\varphi\nabla_\nu\nabla_\beta\varphi \\ & + 6\nabla^\alpha\nabla^\beta\varphi\nabla_\alpha\varphi\nabla_\beta\varphi\nabla_\mu\nabla_\lambda\varphi\nabla_\nu\nabla^\lambda\varphi + 6\nabla^\alpha\nabla^\lambda\varphi\nabla_\beta\varphi\nabla_\lambda\varphi\nabla_\alpha\varphi\nabla^\beta\varphi\nabla_\mu\nabla_\nu\varphi + 2\nabla_\alpha\nabla^\beta\varphi\nabla_\beta\nabla^\lambda\varphi\nabla_\lambda\nabla^\alpha\varphi\nabla_\mu\varphi\nabla_\nu\varphi \\ & + 6\nabla^\alpha\nabla^\beta\varphi\nabla_\alpha\nabla_\beta\varphi\nabla^\lambda\varphi\nabla_\lambda\nabla_{(\mu}\varphi\nabla_{\nu)}\varphi - 12\nabla^\alpha\varphi\nabla_\alpha\nabla_\beta\varphi\nabla^\beta\nabla^\lambda\varphi\nabla_\lambda\nabla_{(\mu}\varphi\nabla_{\nu)}\varphi \\ & - 12\nabla_\alpha\varphi\nabla^\alpha\nabla^\lambda\varphi\nabla^\sigma\varphi\nabla_\lambda\nabla_{(\mu}\varphi\nabla_{\nu)}\nabla_\sigma\varphi + \frac{3}{2}\Box\varphi\left(\nabla_\lambda\varphi\nabla^\lambda\varphi\right)^2R_{\mu\nu} - 3\left(\nabla_\lambda\varphi\nabla^\lambda\varphi\right)^2R_{\sigma(\mu}\nabla_{\nu)}\nabla^\sigma\varphi \\ & + R\left(\nabla_\lambda\varphi\nabla^\lambda\varphi\right)^2\nabla_\mu\nabla_\nu\varphi + 3\Box\varphi\nabla_\lambda\varphi\nabla^\lambda\varphi\nabla^\alpha\varphi\nabla^\beta\varphi\mathcal{W}_{\mu\alpha\nu\beta} - 6\nabla_\lambda\varphi\nabla^\lambda\varphi\nabla^\alpha\varphi\nabla^\beta\nabla^\gamma\varphi\nabla_{(\mu}\varphi\mathcal{W}_{\nu)\beta\alpha\gamma} \\ & + 6\nabla_\lambda\varphi\nabla^\lambda\varphi\nabla^\alpha\varphi\nabla^\beta\varphi\nabla^\gamma\nabla_{(\mu}\varphi\mathcal{W}_{\nu)\alpha\beta\gamma} - 6\nabla_\lambda\varphi\nabla^\lambda\varphi\nabla_\alpha\varphi\nabla^\alpha\nabla_\beta\varphi\nabla_\gamma\varphi\mathcal{W}_{(\mu\ \ \nu)}^{\ \beta\ \ \gamma}\Big],\end{aligned} \tag{2.8}$$

$$\begin{aligned}T^{c_G}_{\mu\nu} = {}& \frac{M_{\rm Pl}}{M^3}c_G\Big[g_{\mu\nu}\left((\Box\varphi)^2 - \nabla_\alpha\nabla_\beta\varphi\nabla^\alpha\nabla^\beta\varphi\right) + 2\nabla_\mu\nabla_\lambda\varphi\nabla_\nu\nabla^\lambda\varphi - 2\Box\varphi\nabla_\mu\nabla_\nu\varphi \\ & + 2R_{\lambda(\mu}\nabla_{\nu)}\varphi\nabla^\lambda\varphi - R^{\alpha\beta}\nabla_\alpha\varphi\nabla_\beta\varphi g_{\mu\nu} + 2\mathcal{W}_{\alpha\mu\beta\nu}\nabla^\alpha\varphi\nabla^\beta\varphi - \frac{2}{3}R\nabla_\mu\varphi\nabla_\nu\varphi + \frac{1}{6}R\nabla^\lambda\varphi\nabla_\lambda\varphi g_{\mu\nu}\Big].\end{aligned} \tag{2.9}$$

The Galileon field equation of motion is given by:

$$0 = c_2\Box\varphi + 2\frac{c_3}{M^3}\left[(\Box\varphi)^2 - \nabla^\alpha\nabla^\beta\varphi\nabla_\alpha\nabla_\beta\varphi - R_{\alpha\beta}\nabla^\alpha\varphi\nabla^\beta\varphi\right]$$

$$
\begin{aligned}
&+\frac{c_4}{M^6}\Big[2(\Box\varphi)^3-6\Box\varphi\nabla_\alpha\nabla_\beta\varphi\nabla^\alpha\nabla^\beta\varphi+4\nabla_\alpha\nabla_\beta\varphi\nabla^\beta\nabla^\gamma\varphi\nabla_\gamma\nabla^\alpha\varphi-\frac{4}{3}R\nabla^\alpha\varphi\nabla^\beta\varphi\nabla_\alpha\nabla_\beta\varphi\\
&-\frac{5}{3}R\Box\varphi\nabla_\lambda\varphi\nabla^\lambda\varphi+4R_{\alpha\beta}\nabla^\alpha\nabla^\beta\varphi\nabla_\lambda\varphi\nabla^\lambda\varphi+4R_{\alpha\beta}\nabla^\alpha\varphi\nabla^\lambda\varphi\nabla^\beta\nabla_\lambda\varphi-2\Box\varphi R_{\alpha\beta}\nabla^\alpha\varphi\nabla^\beta\varphi\\
&+4\mathcal{W}_{\alpha\beta\lambda\rho}\nabla^\alpha\nabla^\lambda\varphi\nabla^\beta\varphi\nabla^\rho\varphi\Big]\\
&+\frac{c_5}{M^9}\Big[(\Box\varphi)^4-6(\Box\varphi)^2\nabla_\alpha\nabla_\beta\varphi\nabla^\alpha\nabla^\beta\varphi+3\left(\nabla_\alpha\nabla_\beta\varphi\nabla^\alpha\nabla^\beta\varphi\right)^2-6\nabla_\alpha\nabla^\rho\varphi\nabla_\beta\nabla_\rho\varphi\nabla^\alpha\nabla^\lambda\varphi\nabla^\beta\nabla_\lambda\varphi\\
&+8\Box\varphi\nabla_\alpha\nabla^\beta\varphi\nabla_\beta\nabla^\lambda\varphi\nabla_\lambda\nabla^\alpha\varphi+6\Box\varphi\nabla_\lambda\varphi\nabla^\lambda\varphi R_{\alpha\beta}\nabla^\alpha\nabla^\beta\varphi-2R(\Box\varphi)^2\nabla_\lambda\varphi\nabla^\lambda\varphi\\
&+\frac{1}{2}RR_{\alpha\beta}\nabla^\alpha\varphi\nabla^\beta\varphi\nabla^\lambda\varphi\nabla_\lambda\varphi-6R_{\alpha\beta}\nabla^\lambda\varphi\nabla_\lambda\varphi\nabla^\alpha\nabla^\sigma\varphi\nabla^\beta\nabla_\sigma\varphi+2R\nabla^\lambda\varphi\nabla_\lambda\varphi\nabla^\alpha\nabla^\beta\varphi\nabla_\alpha\nabla_\beta\varphi\\
&-\frac{3}{2}R_{\rho\sigma}R^{\rho\sigma}\left(\nabla_\lambda\varphi\nabla^\lambda\varphi\right)^2+\frac{1}{4}R^2\left(\nabla_\lambda\varphi\nabla^\lambda\varphi\right)^2+6\Box\varphi\mathcal{W}_{\rho\alpha\sigma\beta}\nabla^\rho\nabla^\sigma\varphi\nabla^\alpha\varphi\nabla^\beta\varphi\\
&+12\mathcal{W}_{\rho\alpha\beta\sigma}\nabla^\rho\nabla^\sigma\varphi\nabla^\beta\nabla^\lambda\varphi\nabla^\alpha\varphi\nabla_\lambda\varphi+3\mathcal{W}_{\rho\alpha\beta\sigma}\nabla^\rho\nabla^\sigma\varphi\nabla^\alpha\nabla^\beta\varphi\nabla^\lambda\varphi\nabla_\lambda\varphi\\
&+6\mathcal{W}_{\alpha\rho\sigma\beta}\nabla^\rho\varphi\nabla^\sigma\varphi\nabla^\alpha\nabla^\lambda\varphi\nabla^\beta\nabla_\lambda\varphi-3\mathcal{W}_{\alpha\rho\beta\sigma}R^{\rho\sigma}\nabla^\alpha\varphi\nabla^\beta\varphi\nabla^\lambda\varphi\nabla_\lambda\varphi\\
&+\frac{3}{2}R_{\mu\alpha\beta\gamma}R_\nu{}^{\alpha\beta\gamma}\nabla^\mu\varphi\nabla^\nu\varphi\nabla^\lambda\varphi\nabla_\lambda\varphi\Big]\\
&+2\frac{M_{\rm Pl}}{M^3}c_GG_{\alpha\beta}\nabla^\alpha\nabla^\beta\varphi. \qquad (2.10)
\end{aligned}
$$

The equations presented in the literature (e.g. [3, 30]) are related to ours via the following Riemann tensor expansion

$$
\begin{aligned}
R_{\mu\nu\alpha\beta}=&\frac{1}{2}\left(g_{\mu\alpha}R_{\nu\beta}+g_{\nu\beta}R_{\mu\alpha}-g_{\mu\beta}R_{\nu\alpha}-g_{\nu\alpha}R_{\mu\beta}\right)\\
&+\mathcal{W}_{\mu\nu\alpha\beta}-\frac{1}{6}R\left(g_{\mu\alpha}g_{\nu\beta}-g_{\mu\beta}g_{\nu\alpha}\right), \qquad (2.11)
\end{aligned}
$$

which cancels some of the terms originally derived in [3]. In Eq. (2.10), we kept only the term proportional to $c_5R_{\mu\alpha\beta\gamma}R_\nu{}^{\alpha\beta\gamma}$ in terms of the Riemann tensor, as using Eq. (2.11) in this particular case would make the equations longer.

2.2 The Perturbation Equations

2.2.1 The Perturbed Equations in General Relativity

In this section, we derive the covariant and gauge invariant perturbation equations in Galileon gravity. This will be done in detail below, but first let us outline the main ingredients of $3+1$ decomposition and their application to GR (which is elegantly described in [37]) for ease of later reference.

The main idea of $3+1$ decomposition is to make spacetime splits of physical quantities with respect to the 4-velocity u^μ of an observer. The projection tensor $h_{\mu\nu}$ is defined by $h_{\mu\nu}=g_{\mu\nu}-u_\mu u_\nu$ and can be used to obtain covariant tensors which live in 3-dimensional hyperspaces perpendicular to u^μ. For example, the covariant spatial derivative $\hat{\nabla}$ of a tensor field $T^{\beta\ldots\gamma}_{\sigma\ldots\lambda}$ is defined as

$$\hat{\nabla}^{\alpha} T^{\beta\cdots\gamma}_{\sigma\cdots\lambda} \equiv h^{\alpha}_{\mu} h^{\beta}_{\nu} \ldots h^{\gamma}_{\kappa} h^{\rho}_{\sigma} \ldots h^{\eta}_{\lambda} \nabla^{\mu} T^{\nu\cdots\kappa}_{\rho\cdots\eta}. \tag{2.12}$$

The energy-momentum tensor and covariant derivative of the 4-velocity are decomposed, respectively, as

$$T_{\mu\nu} = \pi_{\mu\nu} + 2q_{(\mu}u_{\nu)} + \rho u_{\mu}u_{\nu} - p h_{\mu\nu}, \tag{2.13}$$

$$\nabla_{\mu} u_{\nu} = \sigma_{\mu\nu} + \varpi_{\mu\nu} + \frac{1}{3}\theta h_{\mu\nu} + u_{\mu} A_{\nu}, \tag{2.14}$$

where $\pi_{\mu\nu}$ is the projected symmetric and trace-free (PSTF) anisotropic stress, q_{μ} is the heat flux vector, p is the isotropic pressure, ρ is the energy density, $\sigma_{\mu\nu}$ is the PSTF shear tensor, $\varpi_{\mu\nu} = \hat{\nabla}_{[\mu} u_{\nu]}$ is the vorticity, $\theta = \nabla^{\alpha} u_{\alpha} = 3\dot{a}/a = 3H$ (a is the mean expansion scale factor) is the expansion scalar and $A_{\mu} = \dot{u}_{\mu}$; the overdot denotes a time derivative expressed as $\dot{\phi} = u^{\alpha}\nabla_{\alpha}\phi$, brackets mean antisymmetrization and parentheses symmetrization. The normalization is such that $u^{\alpha}u_{\alpha} = 1$. The quantities $\pi_{\mu\nu}$, q_{μ}, ρ and p are referred to as dynamical quantities and $\sigma_{\mu\nu}$, $\varpi_{\mu\nu}$, θ and A_{μ} as kinematical quantities. The dynamical quantities can be obtained from Eq. (2.13) using the relations

$$\begin{aligned} \rho &= T_{\mu\nu} u^{\mu} u^{\nu}, \\ p &= -\frac{1}{3} h^{\mu\nu} T_{\mu\nu}, \\ q_{\mu} &= h^{\nu}_{\mu} u^{\rho} T_{\nu\rho}, \\ \pi_{\mu\nu} &= h^{\rho}_{\mu} h^{\tau}_{\nu} T_{\rho\tau} + p h_{\mu\nu}. \end{aligned} \tag{2.15}$$

Decomposing the Riemann tensor and making use of Einstein equations, we obtain, after linearization, five constraint equations [37]:

$$0 = \hat{\nabla}^{\alpha} \left(\epsilon^{\mu\nu}{}_{\alpha\beta} u^{\beta} \varpi_{\mu\nu} \right), \tag{2.16}$$

$$\kappa q_{\mu} = -\frac{2\hat{\nabla}_{\mu}\theta}{3} + \hat{\nabla}^{\nu}\sigma_{\mu\nu} + \hat{\nabla}^{\nu}\varpi_{\mu\nu}, \tag{2.17}$$

$$\mathcal{B}_{\mu\nu} = \left[\hat{\nabla}^{\alpha}\sigma_{\beta(\mu} + \hat{\nabla}^{\alpha}\varpi_{\beta(\mu} \right] \epsilon_{\nu)\gamma\alpha}{}^{\beta} u^{\gamma}, \tag{2.18}$$

$$\hat{\nabla}^{\nu}\mathcal{E}_{\mu\nu} = \frac{1}{2}\kappa \left[\hat{\nabla}^{\nu}\pi_{\mu\nu} + \frac{2}{3}\theta q_{\mu} + \frac{2}{3}\hat{\nabla}_{\mu}\rho \right], \tag{2.19}$$

$$\hat{\nabla}^{\nu}\mathcal{B}_{\mu\nu} = \frac{1}{2}\kappa \left[\hat{\nabla}_{\alpha} q_{\beta} + (\rho + p)\varpi_{\alpha\beta} \right] \epsilon_{\mu\nu}{}^{\alpha\beta} u^{\nu}; \tag{2.20}$$

and five propagation equations:

$$0 = \dot{\theta} + \frac{1}{3}\theta^2 - \hat{\nabla}\cdot A + \frac{\kappa}{2}(\rho + 3p), \tag{2.21}$$

$$0 = \dot{\sigma}_{\mu\nu} + \frac{2}{3}\theta\sigma_{\mu\nu} - \hat{\nabla}_{\langle\mu}A_{\nu\rangle} + \mathcal{E}_{\mu\nu} + \frac{\kappa}{2}\pi_{\mu\nu}, \tag{2.22}$$

$$0 = \dot{\varpi}_{\mu\nu} + \frac{2}{3}\theta\varpi_{\mu\nu} - \hat{\nabla}_{[\mu}A_{\nu]}, \tag{2.23}$$

$$\begin{aligned} 0 = {} & \frac{\kappa}{2}\left[\dot{\pi}_{\mu\nu} + \frac{1}{3}\theta\pi_{\mu\nu}\right] - \frac{\kappa}{2}\left[(\rho+p)\sigma_{\mu\nu} + \hat{\nabla}_{\langle\mu}q_{\nu\rangle}\right] \\ & - \left[\dot{\mathcal{E}}_{\mu\nu} + \theta\mathcal{E}_{\mu\nu} - \hat{\nabla}^{\alpha}\mathcal{B}_{\beta(\mu}\epsilon_{\nu)\gamma\alpha}{}^{\beta}u^{\gamma}\right], \end{aligned} \tag{2.24}$$

$$\begin{aligned} 0 = {} & \dot{\mathcal{B}}_{\mu\nu} + \theta\mathcal{B}_{\mu\nu} + \hat{\nabla}^{\alpha}\mathcal{E}_{\beta(\mu}\epsilon_{\nu)\gamma\alpha}{}^{\beta}u^{\gamma} \\ & + \frac{\kappa}{2}\hat{\nabla}^{\alpha}\pi_{\beta(\mu}\epsilon_{\nu)\gamma\alpha}{}^{\beta}u^{\gamma}. \end{aligned} \tag{2.25}$$

Here, $\epsilon_{\mu\nu\alpha\beta}$ is the covariant permutation tensor, $\mathcal{E}_{\mu\nu}$ and $\mathcal{B}_{\mu\nu}$ are, respectively, the electric and magnetic parts of the Weyl tensor $\mathcal{W}_{\mu\nu\alpha\beta}$, defined by $\mathcal{E}_{\mu\nu} = u^{\alpha}u^{\beta}\mathcal{W}_{\mu\alpha\nu\beta}$ and $\mathcal{B}_{\mu\nu} = -\frac{1}{2}u^{\alpha}u^{\beta}\epsilon_{\mu\alpha}{}^{\gamma\delta}\mathcal{W}_{\gamma\delta\nu\beta}$. The angle brackets mean taking the trace-free part of a quantity and $\hat{\nabla}\cdot v = \hat{\nabla}^{\alpha}v_{\alpha}$, where v is an arbitrary vector. We note that although there is some level of redundancy in the above equations, one still has enough equations to solve for all the necessary degrees of freedom as we shall see below (we opted to write the redundant equations anyway to maintain the notation of Ref. [37]).

Besides the above equations, it is useful to express the projected Ricci scalar $\hat{R}$ into the hypersurfaces orthogonal to u^{μ} as

$$\hat{R} = 2\kappa\rho - \frac{2}{3}\theta^2. \tag{2.26}$$

The spatial derivative of the projected Ricci scalar, $\eta_{\mu} \equiv a\hat{\nabla}_{\mu}\hat{R}/2$, is given as

$$\eta_{\mu} = \kappa a\hat{\nabla}_{\mu}\rho - \frac{2a}{3}\theta\hat{\nabla}_{\mu}\theta, \tag{2.27}$$

and its propagation equation is given by

$$\dot{\eta}_{\mu} + \frac{2\theta}{3}\eta_{\mu} = -\frac{2a\theta}{3}\hat{\nabla}_{\mu}\hat{\nabla}\cdot A - a\kappa\hat{\nabla}_{\mu}\hat{\nabla}\cdot q. \tag{2.28}$$

Finally, there are the conservation equations for the energy-momentum tensor:

$$\dot{\rho} + (\rho+p)\theta + \hat{\nabla}\cdot q = 0, \tag{2.29}$$

$$\dot{q}_{\mu} + \frac{4}{3}\theta q_{\mu} + (\rho+p)A_{\mu} - \hat{\nabla}_{\mu}p + \hat{\nabla}^{\nu}\pi_{\mu\nu} = 0. \tag{2.30}$$

We always consider the case of a spatially-flat Universe and, as a result, the spatial curvature vanishes at the background level. Thus, setting $\hat{R} = 0$ in Eq. (2.26), we obtain the first Friedmann equation

$$\frac{\theta^2}{3} = \kappa\rho. \tag{2.31}$$

Note that at the background level only the zeroth-order terms contribute to the equations. The second Friedmann equation and the energy-conservation equation are obtained by taking the zeroth-order parts of Eqs. (2.21, 2.29), as

$$\dot{\theta} + \frac{1}{3}\theta^2 + \frac{\kappa}{2}(\rho + 3p) = 0, \tag{2.32}$$

$$\dot{\rho} + (\rho + p)\theta = 0. \tag{2.33}$$

2.2.2 The Perturbation Quantities in Galileon Gravity

In the effective energy-momentum tensor approach, the field equations Eqs. (2.16–2.33) above preserve their forms, but the dynamical quantities ρ, p, q_μ and $\pi_{\mu\nu}$ should be replaced by the effective total ones $\rho^{tot} = \rho^f + \rho^G, p^{tot} = p^f + p^G, q_\mu^{tot} = q_\mu^f + q_\mu^G$ and $\pi_{\mu\nu}^{tot} = \pi_{\mu\nu}^f + \pi_{\mu\nu}^G$, in which the superscripts ^{G} and ^{f} identify the contributions from the Galileon field and the rest of the matter fluid (including cold dark matter, baryons, photons and neutrinos), respectively. From here on we shall drop the superscript ^{tot} for ease of notation.

Before using Eq. (2.15) to calculate ρ^G, p^G, q_μ^G and $\pi_{\mu\nu}^G$ from the components of the Galileon energy-momentum tensor of Eqs. (2.5–2.9), we need an explicit expression for the Ricci tensor $R_{\mu\nu}$ in terms of the kinematical quantities. For this, let us expand the symmetric rank-2 tensor $R_{\mu\nu}$ in the following general way

$$R_{\mu\nu} = \Delta u_\mu u_\nu + \Xi h_{\mu\nu} + 2u_{(\mu}\Upsilon_{\nu)} + \Sigma_{\mu\nu}, \tag{2.34}$$

in which Υ_μ is a four-vector and $\Sigma_{\mu\nu}$ a PSTF rank-2 tensor, both of which live in the 3-dimensional hyperspace perpendicular to the observer's four-velocity ($u^\mu\Upsilon_\mu = u^\mu\Sigma_{\mu\nu} = 0$). Δ and Ξ are scalar quantities. Then, using the modified Einstein field equations

$$R_{\mu\nu} - \frac{1}{2}g_{\mu\nu}R = \kappa T_{\mu\nu}^{tot} = \kappa T_{\mu\nu}^f + \kappa T_{\mu\nu}^G, \tag{2.35}$$

one gets,

$$\Delta = \frac{1}{2}\kappa\,(\rho + 3p)$$

$$= -\left[\dot{\theta} + \frac{1}{3}\theta^2 - \hat{\nabla}\cdot A\right], \tag{2.36}$$

$$\Xi = -\frac{1}{2}\kappa(\rho - p)$$

$$= -\frac{1}{3}\left[\dot{\theta} + \theta^2 + \hat{R} - \hat{\nabla}\cdot A\right], \tag{2.37}$$

$$\Upsilon_\mu = \kappa q_\mu$$

$$= -\frac{2\hat{\nabla}_\mu\theta}{3} + \hat{\nabla}^\nu\sigma_{\mu\nu} + \hat{\nabla}^\nu\varpi_{\mu\nu}, \tag{2.38}$$

$$\Sigma_{\mu\nu} = \kappa\pi_{\mu\nu}$$

$$= -2\left[\dot{\sigma}_{\mu\nu} + \frac{2}{3}\theta\sigma_{\mu\nu} - \hat{\nabla}_{\langle\mu}A_{\nu\rangle} + \mathcal{E}_{\mu\nu}\right]. \tag{2.39}$$

where we have used Eqs. (2.17, 2.21, 2.22, 2.26). Note that the first lines are expressed in terms of total dynamical quantities and the second lines in terms of kinematical quantities.

With the above useful relations and after some tedious but straightforward calculations, the Galileon contribution to the energy-momentum tensor up to first order in perturbed quantities can be identified as

$$\rho^G = c_2\left[\frac{1}{2}\dot{\varphi}^2\right] + \frac{c_3}{M^3}\left[2\dot{\varphi}^3\theta + 2\dot{\varphi}^2\hat{\Box}\varphi\right] + \frac{c_4}{M^6}\left[\frac{5}{2}\dot{\varphi}^4\theta^2 + 4\dot{\varphi}^3\theta\hat{\Box}\varphi + \frac{3}{4}\dot{\varphi}^4\hat{R}\right]$$
$$+ \frac{c_5}{M^9}\left[\frac{7}{9}\dot{\varphi}^5\theta^3 + \frac{5}{3}\dot{\varphi}^4\theta^2\hat{\Box}\varphi + \frac{1}{2}\dot{\varphi}^5\theta\hat{R}\right] + \frac{M_{\rm Pl}}{M^3}c_G\left[\dot{\varphi}^2\theta^2 + \frac{4}{3}\dot{\varphi}\theta\hat{\Box}\varphi + \frac{1}{2}\dot{\varphi}^2\hat{R}\right], \tag{2.40}$$

$$p^G = c_2\left[\frac{1}{2}\dot{\varphi}^2\right] + \frac{c_3}{M^3}\left[-2\ddot{\varphi}\dot{\varphi}^2\right]$$
$$+ \frac{c_4}{M^6}\left[-4\ddot{\varphi}\dot{\varphi}^3\theta - \dot{\varphi}^4\dot{\theta} - \frac{1}{2}\dot{\varphi}^4\theta^2 - 4\ddot{\varphi}\dot{\varphi}^2\hat{\Box}\varphi - \frac{4}{9}\dot{\varphi}^3\theta\hat{\Box}\varphi + \dot{\varphi}^4\hat{\nabla}\cdot A + \frac{1}{12}\dot{\varphi}^4\hat{R}\right]$$
$$+ \frac{c_5}{M^9}\left[-\frac{5}{3}\ddot{\varphi}\dot{\varphi}^4\theta^2 - \frac{2}{3}\dot{\varphi}^5\dot{\theta}\theta - \frac{2}{9}\dot{\varphi}^5\theta^3 - \frac{2}{9}\dot{\varphi}^4\theta^2\hat{\Box}\varphi - \frac{8}{3}\ddot{\varphi}\dot{\varphi}^3\theta\hat{\Box}\varphi - \frac{1}{2}\ddot{\varphi}\dot{\varphi}^4\hat{R} - \frac{2}{3}\dot{\varphi}^4\dot{\theta}\hat{\Box}\varphi + \frac{2}{3}\dot{\varphi}^5\theta\hat{\nabla}\cdot A\right]$$
$$+ \frac{M_{\rm Pl}}{M^3}c_G\left[-\frac{4}{3}\ddot{\varphi}\dot{\varphi}\theta - \frac{2}{3}\dot{\varphi}^2\dot{\theta} - \frac{1}{3}\dot{\varphi}^2\theta^2 + \frac{2}{3}\dot{\varphi}^2\hat{\nabla}\cdot A - \frac{4}{3}\ddot{\varphi}\hat{\Box}\varphi - \frac{4}{9}\dot{\varphi}\theta\hat{\Box}\varphi + \frac{1}{6}\dot{\varphi}^2\hat{R}\right], \tag{2.41}$$

$$q^G_\mu = c_2\left[\dot{\varphi}\hat{\nabla}_\mu\varphi\right] + \frac{c_3}{M^3}\left[2\dot{\varphi}^2\theta\hat{\nabla}_\mu\varphi - 2\dot{\varphi}^2\hat{\nabla}_\mu\dot{\varphi}\right]$$
$$+ \frac{c_4}{M^6}\left[-4\dot{\varphi}^3\theta\hat{\nabla}_\mu\dot{\varphi} + 2\dot{\varphi}^3\theta^2\hat{\nabla}_\mu\varphi - \dot{\varphi}^4\hat{\nabla}_\mu\theta + \frac{3}{2}\dot{\varphi}^4\hat{\nabla}^\alpha\sigma_{\mu\alpha} + \frac{3}{2}\dot{\varphi}^4\hat{\nabla}^\alpha\varpi_{\mu\alpha}\right]$$
$$+ \frac{c_5}{M^9}\left[-\frac{5}{3}\dot{\varphi}^4\theta^2\hat{\nabla}_\mu\dot{\varphi} + \frac{5}{9}\dot{\varphi}^4\theta^3\hat{\nabla}_\mu\varphi - \frac{2}{3}\dot{\varphi}^5\theta\hat{\nabla}_\mu\theta + \dot{\varphi}^5\theta\hat{\nabla}^\alpha\sigma_{\mu\alpha} + \dot{\varphi}^5\theta\hat{\nabla}^\alpha\varpi_{\mu\alpha}\right]$$

$$+\frac{M_{\rm Pl}}{M^3}c_G\left[-\frac{4}{3}\dot\varphi\theta\hat\nabla_\mu\dot\varphi+\frac{2}{3}\dot\varphi\theta^2\hat\nabla_\mu\varphi-\frac{2}{3}\dot\varphi^2\hat\nabla_\mu\theta+\dot\varphi^2\hat\nabla^\alpha\sigma_{\mu\alpha}+\dot\varphi^2\hat\nabla^\alpha\varpi_{\mu\alpha}\right], \tag{2.42}$$

$$\begin{aligned}\pi^G_{\mu\nu}=&\frac{c_4}{M^6}\left[-\ddot\varphi^4\left(\dot\sigma_{\mu\nu}-\hat\nabla_{\langle\mu}A_{\nu\rangle}-\mathcal{E}_{\mu\nu}\right)-\left(6\dddot\varphi\dot\varphi^2+\frac{2}{3}\ddot\varphi^3\theta\right)\hat\nabla_{\langle\mu}\hat\nabla_{\nu\rangle}\varphi-\left(6\dddot\varphi\ddot\varphi^3+\frac{4}{3}\ddot\varphi^4\theta\right)\sigma_{\mu\nu}\right]\\&+\frac{c_5}{M^9}\left[-\left(\dot\varphi^5\dot\theta+\dot\varphi^5\theta^2+6\dddot\varphi\ddot\varphi^4\theta\right)\sigma_{\mu\nu}-\left(\dot\varphi^5\theta+3\dddot\varphi\ddot\varphi^4\right)\dot\sigma_{\mu\nu}\right.\\&\left.-\left(4\dddot\varphi\ddot\varphi^3\theta+\dot\varphi^4\dot\theta+\frac{1}{3}\ddot\varphi^4\theta^2\right)\hat\nabla_{\langle\mu}\hat\nabla_{\nu\rangle}\varphi+\left(\dot\varphi^5\theta+3\dddot\varphi\ddot\varphi^4\right)\hat\nabla_{\langle\mu}A_{\nu\rangle}-6\dddot\varphi\ddot\varphi^4\mathcal{E}_{\mu\nu}\right]\\&+\frac{M_{\rm Pl}}{M^3}c_G\left[-\left(2\dddot\varphi\ddot\varphi+\frac{2}{3}\ddot\varphi^2\theta\right)\sigma_{\mu\nu}-\left(\frac{2}{3}\ddot\varphi\theta+2\dddot\varphi\right)\hat\nabla_{\langle\mu}\hat\nabla_{\nu\rangle}\varphi+2\ddot\varphi^2\mathcal{E}_{\mu\nu}\right],\end{aligned} \tag{2.43}$$

in which $\hat\Box\equiv\hat\nabla^\mu\hat\nabla_\mu$.

Following the same procure, the Galileon field equation of motion, Eq. (2.10), is given by

$$\begin{aligned}0=&c_2\left[\dddot\varphi+\hat\Box\varphi+\ddot\varphi\theta\right]+\frac{c_3}{M^3}\left[4\dddot\varphi\ddot\varphi\theta+\frac{8}{3}\ddot\varphi\theta\hat\Box\varphi+4\dddot\varphi\hat\Box\varphi+2\ddot\varphi^2\theta^2+2\ddot\varphi^2\dot\theta-2\ddot\varphi^2\hat\nabla\cdot A\right]\\&+\frac{c_4}{M^6}\left[6\dddot\varphi\ddot\varphi^2\theta^2+4\ddot\varphi^3\dot\theta\theta+2\ddot\varphi^3\theta^3+8\dddot\varphi\ddot\varphi\theta\hat\Box\varphi+\frac{26}{9}\ddot\varphi^2\theta^2\hat\Box\varphi\right.\\&\left.-4\ddot\varphi^3\theta\hat\nabla\cdot A+4\ddot\varphi^2\dot\theta\hat\Box\varphi+3\dddot\varphi\ddot\varphi^2\hat R+\frac{1}{3}\ddot\varphi^3\theta\hat R\right]\\&+\frac{c_5}{M^9}\left[\frac{5}{9}\ddot\varphi^4\theta^4+\frac{20}{9}\dddot\varphi\ddot\varphi^3\theta^3+\frac{5}{3}\ddot\varphi^4\dot\theta\theta^2+\frac{8}{9}\ddot\varphi^3\theta^3\hat\Box\varphi+\frac{1}{2}\ddot\varphi^4\dot\theta\hat R\right.\\&\left.+\frac{1}{6}\ddot\varphi^4\theta^2\hat R-\frac{5}{3}\ddot\varphi^4\theta^2\hat\nabla\cdot A+4\dddot\varphi\ddot\varphi^2\theta^2\hat\Box\varphi+\frac{8}{3}\ddot\varphi^3\dot\theta\theta\hat\Box\varphi+2\dddot\varphi\ddot\varphi^3\theta\hat R\right]\\&+\frac{M_{\rm Pl}}{M^3}c_G\left[\frac{2}{3}\dddot\varphi\theta^2+\frac{4}{3}\dot\theta\hat\Box\varphi+\frac{2}{3}\theta^2\hat\Box\varphi+\frac{4}{3}\ddot\varphi\dot\theta\theta+\frac{2}{3}\ddot\varphi\theta^3-\frac{4}{3}\ddot\varphi\theta\hat\nabla\cdot A+\dddot\varphi\hat R+\frac{1}{3}\ddot\varphi\theta\hat R\right].\end{aligned} \tag{2.44}$$

As a consistency test, we checked that Eqs. (2.40–2.43) satisfy the conservation Eqs. (2.29, 2.30).

2.2.3 *Perturbed Equations in k-space*

For the purpose of the numerical studies presented in this chapter, we need to write the perturbed quantities derived in the last subsection in terms of k-space variables. This is achieved with the aid of the following harmonic definitions:

$$\hat{\nabla}_\mu\varphi \equiv \sum_k \frac{k}{a}\gamma Q^k_\mu, \quad \hat{\nabla}_\mu\theta \equiv \sum_k \frac{k^2}{a^2}\mathcal{Z}Q^k_\mu,$$
$$A_\mu \equiv \sum_k \frac{k}{a}AQ^k_\mu, \quad \hat{\nabla}_\mu\rho \equiv \sum_k \frac{k}{a}\chi Q^k_\mu,$$
$$\pi_{\mu\nu} \equiv \sum_k \Pi Q^k_{\mu\nu}, \quad \sigma_{\mu\nu} \equiv \sum_k \frac{k}{a}\sigma Q^k_{\mu\nu},$$
$$\eta_\mu \equiv \sum_k \frac{k^3}{a^2}\eta Q^k_\mu, \quad \mathcal{E}_{\mu\nu} \equiv -\sum_k \frac{k^2}{a^2}\phi Q^k_{\mu\nu}, \tag{2.45}$$

in which Q^k is the eigenfunction of the comoving spatial Laplacian $a^2\hat{\Box}$ satisfying

$$\hat{\Box}Q^k = \frac{k^2}{a^2}Q^k, \tag{2.46}$$

and Q^k_μ and $Q^k_{\mu\nu}$ are given by $Q^k_\mu = \frac{a}{k}\hat{\nabla}_\mu Q^k$ and by $Q^k_{\mu\nu} = \frac{a}{k}\hat{\nabla}_{\langle\mu}Q_{\nu\rangle}$, respectively.

In terms of these harmonic expansion variables, Eqs. (2.17, 2.19, 2.22, 2.24, 2.27, 2.28) can be rewritten as

$$\frac{2}{3}k^2(\sigma - \mathcal{Z}) = \kappa q a^2, \tag{2.47}$$
$$k^3\phi = -\frac{1}{2}\kappa a^2\left[k(\Pi + \chi) + 3\mathcal{H}q\right], \tag{2.48}$$
$$k(\sigma\prime + \mathcal{H}\sigma) = k^2(\phi + A) - \frac{1}{2}\kappa a^2\Pi, \tag{2.49}$$
$$k^2(\phi' + \mathcal{H}\phi) = \frac{1}{2}\kappa a^2\left[k(\rho + p)\sigma + kq - \Pi' - \mathcal{H}\Pi\right], \tag{2.50}$$
$$k^2\eta = \kappa\chi a^2 - 2k\mathcal{H}\mathcal{Z}, \tag{2.51}$$
$$k\eta\prime = -\kappa q a^2 - 2k\mathcal{H}A, \tag{2.52}$$

respectively, where $\mathcal{H} = a'/a$ and a prime denotes a derivative with respect to conformal time τ ($ad\tau = dt$, with t the physical time). From Eqs. (2.40, 2.42, 2.43) one obtains the k-space variables χ^G, q^G and Π^G

$$\begin{aligned}\chi^G = {} & c_2\frac{1}{a^2}\left(\varphi'\gamma' + \varphi'^2A\right) + \frac{c_3}{M^3}\frac{1}{a^4}\left(\left[18\varphi'^2\mathcal{H}\gamma' + 18\varphi'^3\mathcal{H}A\right] + k\left[2\varphi'^3\mathcal{Z}\right] + k^2\left[2\varphi'^2\gamma\right]\right)\\
& + \frac{c_4}{M^6}\frac{1}{a^6}\left(\left[90\varphi'^3\mathcal{H}^2\gamma' + 90\varphi'^4\mathcal{H}^2A\right] + k\left[15\varphi'^4\mathcal{H}\mathcal{Z}\right] + k^2\left[12\varphi'^3\mathcal{H}\gamma + \frac{3}{2}\varphi'^4\eta\right]\right)\\
& + \frac{c_5}{M^9}\frac{1}{a^8}\left(\left[105\varphi'^4\mathcal{H}^3\gamma' + 105\varphi'^5\mathcal{H}^3A\right] + k\left[21\varphi'^5\mathcal{H}^2\mathcal{Z}\right] + k^2\left[15\varphi'^4\mathcal{H}^2\gamma + 3\varphi'^5\mathcal{H}\eta\right]\right)\\
& + \frac{M_{\rm Pl}}{M^3}c_G\frac{1}{a^4}\left(\left[18\varphi'\mathcal{H}^2\gamma' + 18\varphi'^2\mathcal{H}^2A\right] + k\left[6\varphi'^2\mathcal{H}\mathcal{Z}\right] + k^2\left[4\varphi'\mathcal{H}\gamma + \varphi'^2\eta\right]\right),\end{aligned} \tag{2.53}$$

$$
\begin{aligned}
q^G = {} & c_2 \frac{k}{a^2}\left(\varphi'\gamma\right) + \frac{c_3}{M^3}\frac{k}{a^4}\left(6\varphi'^2\mathcal{H}\gamma - 2\varphi'^2\gamma' - 2\varphi'^3 A\right) \\
& + \frac{c_4}{M^6}\frac{1}{a^6}\left(k\left[-12\varphi'^3\mathcal{H}\gamma' - 12\varphi'^4\mathcal{H}A + 18\varphi'^3\mathcal{H}^2\gamma\right] + k^2\left[\varphi'^4\sigma - \varphi'^4\mathcal{Z}\right]\right) \\
& + \frac{c_5}{M^9}\frac{1}{a^8}\left(k\left[-15\varphi'^4\mathcal{H}^2\gamma' - 15\varphi'^5\mathcal{H}^2 A + 15\varphi'^4\mathcal{H}^3\gamma\right] + 2k^2\left[-\varphi'^5\mathcal{H}\mathcal{Z} + \varphi'^5\mathcal{H}\sigma\right]\right) \\
& + \frac{M_{\rm Pl}}{M^3}c_G\frac{1}{a^4}\left(k\left[-4\varphi'\mathcal{H}\gamma' - 4\varphi'^2\mathcal{H}A + 6\varphi'\mathcal{H}^2\gamma\right] + \frac{2}{3}k^2\left[\varphi'^2\sigma - \varphi'^2\mathcal{Z}\right]\right),
\end{aligned}
\tag{2.54}
$$

$$
\begin{aligned}
\Pi^G = {} & \frac{c_4}{M^6}\frac{1}{a^6}\left(k\left[-\varphi'^4\sigma' + 3\varphi'^4\mathcal{H}\sigma - 6\varphi''\varphi'^3\sigma\right] + k^2\left[4\varphi'^3\mathcal{H}\gamma - 6\varphi''\varphi'^2\gamma + \varphi'^4 A - \varphi'^4\phi\right]\right) \\
& + \frac{c_5}{M^9}\frac{1}{a^8}\left(k\left[-3\varphi'^5\mathcal{H}'\sigma + 12\varphi'^5\mathcal{H}^2\sigma - 15\varphi''\varphi'^4\mathcal{H}\sigma - 3\varphi''\varphi'^4\sigma'\right]\right. \\
& \left. + k^2\left[-12\varphi''\varphi'^3\mathcal{H}\gamma + 12\varphi'^4\mathcal{H}^2\gamma - 3\varphi'^4\mathcal{H}'\gamma + 3\varphi''\varphi'^4 A + 6\varphi''\varphi'^4\phi - 6\varphi'^5\mathcal{H}\phi\right]\right) \\
& + \frac{M_{\rm Pl}}{M^3}c_G\frac{1}{a^4}\left(k\left[-2\varphi''\varphi'\sigma\right] - 2k^2\left[\varphi''\gamma + \varphi'^2\phi\right]\right).
\end{aligned}
\tag{2.55}
$$

Note that the spatial derivative of the isotropic pressure p in k-space is not needed in the CAMB code, which is why we do not write it here. Finally, in k-space, the perturbed Galileon field equation of motion, Eq. (2.44), reads

$$
\begin{aligned}
0 = {} & \frac{c_2}{a^3}\left(k\left[\gamma'' + 2\gamma'\mathcal{H} + \varphi' A' + \varphi'\mathcal{H}A + 2\varphi'' A\right] + k^2\varphi'\mathcal{Z} + k^3\gamma\right) \\
& + \frac{c_3}{M^3}\frac{1}{a^5}\left(k\left[12\gamma''\varphi'\mathcal{H} + 12\varphi'^2\mathcal{H}A' - 18\varphi'^2\mathcal{H}^2 A + 36\varphi''\varphi'\mathcal{H}A + 12\varphi''\mathcal{H}\gamma' + 12\varphi'\mathcal{H}'\gamma' + 18\varphi'^2\mathcal{H}' A\right]\right. \\
& \left. + k^2\left[6\varphi'^2\mathcal{H}\mathcal{Z} + 2\varphi'^2\mathcal{Z}' + 4\varphi''\varphi'\mathcal{Z}\right] + k^3\left[4\varphi'\mathcal{H}\gamma - 2\varphi'^2 A + 4\varphi''\gamma\right]\right) \\
& + \frac{c_4}{M^6}\frac{1}{a^7}\left(k\left[54\varphi'^2\mathcal{H}^2\gamma'' - 108\varphi'^2\mathcal{H}^3\gamma' + 54\varphi'^3\mathcal{H}^2 A' - 198\varphi'^3\mathcal{H}^3 A + 216\varphi''\varphi'^2\mathcal{H}^2 A + 108\varphi''\varphi'\mathcal{H}^2\gamma'\right.\right. \\
& \left. + 108\varphi'^2\mathcal{H}\mathcal{H}'\gamma' + 144\varphi'^3\mathcal{H}\mathcal{H}' A\right] + k^2\left[-6\varphi'^3\mathcal{H}^2\mathcal{Z} + 36\varphi''\varphi'^2\mathcal{H}\mathcal{Z} + 12\varphi'^3\mathcal{H}'\mathcal{Z} + 12\varphi'^3\mathcal{H}\mathcal{Z}'\right] \\
& \left. + k^3\left[-10\varphi'^2\mathcal{H}^2\gamma - 12\varphi'^3\mathcal{H}A - 4\varphi'^3\mathcal{H}\eta + 24\varphi''\varphi'\mathcal{H}\gamma + 12\varphi'^2\mathcal{H}'\gamma + 6\varphi''\varphi'^2\eta\right]\right) \\
& + \frac{c_5}{M^9}\frac{1}{a^9}\left(k\left[-240\varphi'^3\mathcal{H}^4\gamma' - 345\varphi'^4\mathcal{H}^4 A + 60\varphi'^3\mathcal{H}^3\gamma'' + 60\varphi'^4\mathcal{H}^3 A' + 300\varphi''\varphi'^3\mathcal{H}^3 A + 180\varphi''\varphi'^2\mathcal{H}^3\gamma'\right.\right. \\
& \left. + 180\varphi'^3\mathcal{H}^2\mathcal{H}'\gamma' + 225\varphi'^4\mathcal{H}^2\mathcal{H}' A\right] + k^2\left[-45\varphi'^4\mathcal{H}^3\mathcal{Z} + 60\varphi''\varphi'^3\mathcal{H}^2\mathcal{Z} + 15\varphi'^4\mathcal{H}^2\mathcal{Z}' + 30\varphi'^4\mathcal{H}\mathcal{H}'\mathcal{Z}\right] \\
& \left. + k^3\left[-36\varphi'^3\mathcal{H}^3\gamma - 12\varphi'^4\mathcal{H}^2\eta - 15\varphi'^4\mathcal{H}^2 A + 3\varphi'^4\mathcal{H}'\eta + 36\varphi''\varphi'^2\mathcal{H}^2\gamma + 24\varphi'^3\mathcal{H}\mathcal{H}'\gamma + 12\varphi''\varphi'^3\mathcal{H}\eta\right]\right) \\
& + \frac{M_{\rm Pl}}{M^3}\frac{c_G}{a^5}\left(k\left[6\mathcal{H}^2\gamma'' + 6\varphi'\mathcal{H}^2 A' - 18\varphi'\mathcal{H}^3 A + 12\varphi''\mathcal{H}^2 A + 12\mathcal{H}\mathcal{H}'\gamma' + 24\varphi'\mathcal{H}\mathcal{H}' A\right]\right. \\
& \left. + k^2\left[6\varphi'\mathcal{H}^2\mathcal{Z} + 4\varphi''\mathcal{H}\mathcal{Z} + 4\varphi'\mathcal{H}\mathcal{Z}' + 4\varphi'\mathcal{H}'\mathcal{Z}\right] + k^3\left[2\mathcal{H}^2\gamma - 4\varphi'\mathcal{H}A + 4\mathcal{H}'\gamma + 2\varphi''\eta\right]\right).
\end{aligned}
\tag{2.56}
$$

As another consistency test, we have checked that the conservation Eqs. (2.29, 2.30) in k-space,

$$
\chi' + (k\mathcal{Z} - 3\mathcal{H}A)(\rho + p) + 3\mathcal{H}(\chi + \chi^p) + kq = 0,
\tag{2.57}
$$

$$q' + 4\mathcal{H}q + (\rho + p)kA - k\chi^p + \frac{2}{3}k\Pi = 0, \tag{2.58}$$

are satisfied by the k-space perturbed expressions derived above.

Synchronous and Newtonian Gauge Equations

Here, we present the recipe to write the CGI perturbation equations in the synchronous and in the newtonian gauge [38].

The perturbed Friedmann-Robertson-Walker line element in the synchronous gauge is written as

$$ds^2{}_S = a^2(\tau)\left[d\tau^2 - (\delta_{ij} + h^S_{ij})dx^i dx^j\right]. \tag{2.59}$$

Latin indices run over 1, 2 and 3, δ_{ij} is the delta function and the spatial perturbed metric $h^S_{ij} \equiv h^S_{ij}(\mathbf{x}, \tau)$ is given by

$$h^S_{ij} = \int d^3k\, e^{i\mathbf{kx}} \left[\hat{k}_i\hat{k}_j h^S(\mathbf{k}, \tau) + 6\left(\hat{k}_i\hat{k}_j - \frac{1}{3}\delta_{ij}\right)\eta^S(\mathbf{k}, \tau)\right], \tag{2.60}$$

where a superscript ^{S} denotes quantities in the synchronous gauge, $\mathbf{x}$ is the spatial position vector and $\hat{k} = \mathbf{k}/k$ is the unit vector mode in the $\mathbf{k}$-direction. The CGI and the synchronous gauge quantities are related by means of the following relations

$$\begin{aligned}
\phi &= \frac{1}{4k^2}\left[6\eta''^S + h''^S\right] - \frac{1}{4}\eta^S,\\
A &= 0,\\
\eta &= -2\eta^S,\\
\mathcal{Z} &= \frac{h'^S}{2k},\\
\sigma &= \frac{1}{2k}\left(6\eta'^S + h'^S\right).
\end{aligned} \tag{2.61}$$

The line element in the Newtonian (also known as longitudinal) gauge is diagonal, described by two scalar potentials Ψ and Φ, and reads

$$ds^2_N = a^2(\tau)\left[(1 + 2\Psi)d\tau^2 - (1 - 2\Phi)dx^i dx_i\right]. \tag{2.62}$$

Written in this way, the perturbed line element is only applicable to the study of the scalar modes of the metric perturbations. The two potentials are related to the Weyl potential ϕ as

$$\Psi = \phi - \frac{1}{2}\left(\frac{a}{k}\right)^2 \kappa\Pi,$$

$$\Phi = \phi + \frac{1}{2}\left(\frac{a}{k}\right)^2 \kappa\Pi, \tag{2.63}$$

and the other CGI quantities are given by

$$\begin{aligned} A &= -\Psi, \\ \eta &= -2\Phi, \\ \mathcal{Z} &= -\frac{3}{k}\left(\Phi' + \Psi\mathcal{H}\right), \\ \sigma &= 0. \end{aligned} \tag{2.64}$$

We do not present the full perturbed field equations in the synchronous and Newtonian gauges because they are not used in the `CAMB` code [43], which is the code we modify to follow the cosmology of the Galileon model. However, note that `CAMB` works in the cold-dark-matter frame where $A = 0$, which is equivalent to the synchronous gauge written in a slightly different formalism.

2.3 Understanding the Galileon Parameter Space: Free Parameters and Stability Conditions

Before proceeding to showing the results, it is useful to analyse the equations of the model to determine which of the new parameters are actually extra parameters and which are derived ones. In this section, we also present two different approaches to obtain the background evolution. The first one involves integrating numerically the equations of the model, whereas the second approach makes use of analytical formulae that characterizes the so-called *tracker solution*. We comment also on the conditions for the avoidance of ghost and Laplace instabilities in the scalar sector of the model.

A main goal of this section is to present a concise description of some key aspects of the equations of the model, for ease of later reference. For this reason, in this section we take $c_G = 0$, as we do in all the other chapters. The inclusion of c_G in the considerations of this section is nevertheless straightforward.

2.3.1 Scaling Degeneracy

By looking at Eqs. (2.40–2.44), we note that they are invariant under the following transformations:

$$\begin{aligned} c_2 &\longrightarrow c_2' = c_2/B^2, \\ c_3 &\longrightarrow c_3' = c_3/B^3, \\ c_4 &\longrightarrow c_4' = c_4/B^4, \end{aligned}$$

$$c_5 \longrightarrow c_5' = c_5/B^5,$$
$$\varphi \longrightarrow \varphi' = \varphi B, \tag{2.65}$$

in which B is an arbitrary constant and the transformation of φ holds for both the background and perturbation parts. The reason for this scaling lies in the fact that each of the Galileon Lagrangians $\mathcal{L}_i$ yields terms which all have the same power in the Galileon field φ (for the counting of the power, the time and spatial derivatives of φ are treated equally as φ).

From a practical point of view, the scaling of the Galileon field φ is realized by rescaling its time derivative at the initial redshift, z_i, when the calculation starts, $\dot{\varphi}_i = \dot{\varphi}(z = z_i)$.[3] As a result, according to Eq. (2.65), the impact of smaller values of $\dot{\bar{\varphi}}_i$ can always be compensated by larger values of the c_n parameters and vice versa. This makes the c_n parameters unbounded, thus preventing proper constraints on the parameter space. A possible way to break the scaling degeneracy is to use one of the Galileon parameters as a reference to write down invariant quantities under the scaling. For instance, taking c_3 as the reference parameter, then the invariant quantities are

$$\left\{ \frac{c_2}{c_3^{2/3}}, \frac{c_4}{c_3^{4/3}}, \frac{c_5}{c_3^{5/3}}, c_3^{1/3} \dot{\bar{\varphi}}_i \right\}. \tag{2.66}$$

The above equations make it explicit that the need to break the scaling degeneracy reduces the dimensionality of the parameter space of the model by one. Another approach could be to fix the value of c_2, so as to normalize the canonical kinetic term of the theory.

2.3.2 *Tracker Solution*

The background energy and pressure densities of the Galileon field that enter Eqs. (2.31) and (2.32) are given by taking the zeroth-order part (non-hatted terms) of Eqs. (2.40) and (2.41), respectively, as

[3] In principle, to achieve the exact scaling at the linear perturbation level, one has to resize the Galileon field perturbation $\delta\varphi_i$ and its time derivative $\dot{\delta\varphi}_i$ as well. However, our choices of initial conditions are $\delta\varphi_i = \dot{\delta\varphi}_i = 0$, which means that the resizing does not need to be done explicitly. We have checked that our results are insensitive to sufficiently small changes around these initial values for all length scales (or k-modes) that are of interest to us. Here, 'sufficiently small' means small enough to be still in the regime of linear perturbation theory. Typically, such a condition is quoted as $\delta\varphi_i \ll \bar{\varphi}_i$. However, the background value of the field is irrelevant in the covariant Galileon model since the background equations only involve $\dot{\bar{\varphi}}$ and $\ddot{\bar{\varphi}}$ and not $\bar{\varphi}$. As an alternative, we adopt $\delta\varphi_i \ll \dot{\bar{\varphi}}_i/H_i$ as a criterion for the validity of the linear perturbation analysis. This restricts $\delta\varphi_i$ and $\dot{\delta\varphi}_i$ to be so small that it makes no practical difference if they are set to be exactly zero.

$$\bar{\rho}_\varphi = c_2\left[\frac{1}{2}\dot{\varphi}^2\right] + \frac{c_3}{M^3}\left[2\dot{\varphi}^3\theta\right] + \frac{c_4}{M^6}\left[\frac{5}{2}\dot{\varphi}^4\theta^2\right] + \frac{c_5}{M^9}\left[\frac{7}{9}\dot{\varphi}^5\theta^3\right], \tag{2.67}$$

$$\begin{aligned}\bar{p}_\varphi = c_2\left[\frac{1}{2}\dot{\varphi}^2\right] - \frac{c_3}{M^3}\left[2\ddot{\varphi}\dot{\varphi}^2\right] + \frac{c_4}{M^6}\left[-4\ddot{\varphi}\dot{\varphi}^3\theta - \dot{\varphi}^4\dot{\theta} - \frac{1}{2}\dot{\varphi}^4\theta^2\right] \\ + \frac{c_5}{M^9}\left[-\frac{5}{3}\ddot{\varphi}\dot{\varphi}^4\theta^2 - \frac{2}{3}\dot{\varphi}^5\dot{\theta}\theta - \frac{2}{9}\dot{\varphi}^5\theta^3\right].\end{aligned} \tag{2.68}$$

Similarly, the background part of the equation of motion of the Galileon field is given by

$$\begin{aligned}0 = c_2\left[\ddot{\varphi} + \dot{\varphi}\theta\right] + \frac{c_3}{M^3}\left[4\ddot{\varphi}\dot{\varphi}\theta + 2\dot{\varphi}^2\theta^2 + 2\dot{\varphi}^2\dot{\theta}\right] + \frac{c_4}{M^6}\left[6\ddot{\varphi}\dot{\varphi}^2\theta^2 + 4\dot{\varphi}^3\dot{\theta}\theta + 2\dot{\varphi}^3\theta^3\right] \\ + \frac{c_5}{M^9}\left[\frac{5}{9}\dot{\varphi}^4\theta^4 + \frac{20}{9}\ddot{\varphi}\dot{\varphi}^3\theta^3 + \frac{5}{3}\dot{\varphi}^4\dot{\theta}\theta^2\right].\end{aligned} \tag{2.69}$$

The above equation and Eq. (2.31) or (2.32) can be solved numerically from some initial redshift, z_i, until the present day, $z = 0$. Reference [39] did this and showed that different initial conditions of the background Galileon field derivative, $\dot{\varphi}_i$, give rise to different time evolution that eventually merge into a common trajectory called the *tracker solution*. The advantage of assuming that the Galileon model follows the tracker at all times is twofold. First, it allows one to derive analytical formulae for the background evolution (just like, e.g., ΛCDM models), which greatly simplifies and speeds up the numerical calculations; second, it also allows us to reduce the number of free parameters by one, which is helpful when exploring the high-dimensional parameter space of the model. Next, we show these two advantages explicitly.

The tracker evolution is characterized by [39]

$$H\dot{\tilde{\varphi}} = \text{constant} \equiv \xi H_0^2, \tag{2.70}$$

where ξ is a dimensionless constant. Multiplying Eq. (2.31) by H^2, eliminating $\dot{\tilde{\varphi}}$ with Eq. (2.70) and dividing the resulting equation by H_0^4, one obtains

$$\begin{aligned}E^4 = \left(\Omega_{r0}a^{-4} + \Omega_{m0}a^{-3} + \Omega_{\nu 0}\frac{\bar{\rho}_\nu(a)}{\bar{\rho}_{\nu 0}}\right)E^2 \\ + \frac{1}{6}c_2\xi^2 + 2c_3\xi^3 + \frac{15}{2}c_4\xi^4 + 7c_5\xi^5,\end{aligned} \tag{2.71}$$

in which $E \equiv H/H_0$, $\Omega_{i0} = \bar{\rho}_{i0}/\rho_{c0}$, where $\rho_{c0} = 3H_0^2/\kappa$ is the critical energy density today. The subscript $_r$ refers to radiation, $_m$ to baryonic and cold dark matter and $_\nu$ refers to neutrinos (the function $\bar{\rho}_\nu(a)$ describes the time evolution of the neutrino density, which depends on neutrino mass). At the present day, Eq. (2.71) gives

$$\Omega_{\varphi 0} \equiv 1 - \Omega_{r0} - \Omega_{m0} - \Omega_{\nu 0} = \frac{1}{6}c_2\xi^2 + 2c_3\xi^3 + \frac{15}{2}c_4\xi^4 + 7c_5\xi^5, \quad (2.72)$$

where we have assumed spatial flatness (as everywhere in this thesis). This equation can be regarded as a constraint equation for one of the Galileon parameters, i.e., one of the parameters can be fixed by the condition that the Universe is spatially flat. The assumption that the field follows the tracker allows us to fix one more Galileon parameter. This second constraint equation can be obtained by plugging Eq. (2.70) into Eq. (2.69), which yields

$$c_2\xi^2 + 6c_3\xi^3 + 18c_4\xi^4 + 15c_5\xi^5 = 0. \quad (2.73)$$

Equation (2.71) is a second-order algebraic equation for $E(a)$, whose solution reads

$$E(a)^2 = \frac{1}{2}\left[\left(\Omega_{r0}a^{-4} + \Omega_{m0}a^{-3} + \Omega_{\nu 0}\frac{\bar{\rho}_\nu(a)}{\bar{\rho}_{\nu 0}}\right) + \sqrt{\left(\Omega_{r0}a^{-4} + \Omega_{m0}a^{-3} + \Omega_{\nu 0}\frac{\bar{\rho}_\nu(a)}{\bar{\rho}_{\nu 0}}\right)^2 + 4\Omega_{\varphi 0}}\right]. \quad (2.74)$$

Finally, using Eq. (2.70) we have

$$\dot{\bar{\varphi}} = \xi H_0 / E(a). \quad (2.75)$$

These last two equations completely specify the tracker background evolution in the Galileon model. Note that in our treatment of the tracker solution, one essentially replaces $\dot{\bar{\varphi}}_i$ by ξ in our notation, as can be checked by evaluating Eq. (2.75) at z_i. We stress, however, that one must first check whether the tracker solution is favoured by the observational data before comfortably using it in studies of the Galileon model. This check shall be done explicitly in the next chapter.

In summary, by assuming the (i) tracker solution and that (ii) the Universe is spatially flat, together with the (iii) need to break the scaling degeneracy, one is able to reduce the dimensionality of the parameter space of the Galileon model by three.

2.3.3 *Stability Conditions*

In the next chapter, we present observational constraints on the Galileon model. However, the parameter space can be constrained a priori by the requirement to avoid the appearance of theoretical instabilities. The Galileon Lagrangian, being a subset of the more general Horndeski Lagrangian, is automatically protected against the propagation of Ostrogradsky ghosts as the equations are retained up to second order [11]. However, other sorts of theoretical pathologies may still arise.

In all our discussions about the Galileon model, we consider the conditions for each point in parameter space not to develop ghost degrees of freedom or Laplace instabilities in the scalar sector of the linear perturbations. We do not present a detailed derivation of these stability conditions, but refer the reader to Refs. [30, 40, 41] where these have been derived and discussed. The analytical method to derive these conditions is different in between Refs. [40, 41] and [30]. However, we have checked that the two formulae consistenly identify which regions of the parameter space are unstable (the reader can sneak a peak at Fig. 3.12). The no-ghost and no-Laplace stability conditions, despite applying to the scalar perturbations, depend only on background quantities. Hence, in our calculations, we first solve the background evolution to test whether or not a given set of parameters is stable. The calculation of the evolution of the perturbations is only performed if the point is theoretically viable. We only test the theoretical stability of any given point in the past, since there is no evidence that the instabilities cannot develop in the unprobed future.

One could also consider other theoretical conditions such as those which ensure that the Galileon field perturbation does not propagate superluminally (i.e. $c_s^2 > 1$). However, such cases do not necessarily imply the existence of pathologies such as the violation of causality (see e.g. [42]) and therefore we do not employ them. We also do not rule out a priori cases where $\bar{\rho}_\varphi < 0$ at some point in time, but instead let the data decide their viability.

2.4 Results

In this section we present and discuss our results. These were obtained with a suitably modified version of the `CAMB` code [43] to follow Galileon gravity models.

2.4.1 Background

In the remainder of this chapter, we compute the evolution of the cosmological background numerically (without enforcing the tracker solution) using the Friedmann equation, Eq. (2.32), and the background Galileon equation of motion, Eq. (2.69).[4] The value of the Galileon background energy density $\bar{\rho}_{\varphi,i}$ at the starting redshift, which we take to be $z_i = 10^6$, is determined through Eq. (2.67) by the initial values of the field time derivative $\dot{\varphi}_i$ and the expansion rate θ_i. The latter is given by the fixed matter and radiation components via Eq. (2.31) (the Galileon background energy density is negligible at early times). We specify θ_i using $\Omega_{m0} = 0.265$ and $\Omega_{r0} \approx 8 \times 10^{-5}$ for the present day values of the fractional energy density of matter and

[4]Recall that if $c_G \neq 0$, then the equations presented in the last section should be augmented with the c_G contribution. This can be done straightforwardly by reading the background part of the c_G terms from the relevant equations.

radiation, respectively [44, 45]. Since we are assuming a spatially flat Universe we need the evolution of the Galileon field to be such that $\Omega_{\varphi 0} \approx 1 - \Omega_{m0} \approx 0.735$. In the previous section, we have seen that on the tracker, the flatness condition results in the constraint of Eq. (2.72). When solving the equations numerically, the strategy is to 'tune' the value of one of the Galileon parameters by a trial and error approach. In this chapter, we choose to tune c_2. As a consistency test, we have checked that Eqs. (2.31, 2.33) are satisfied by the numerical solution we obtain from `CAMB`. Moreover, we have also checked that the background expansion history from `CAMB` agrees very well with those in the literature [30, 39, 46–49] and from an independent code written in `Python` by us.

We focus on four different sets of Galileon parameters which we list in Table 2.1. In [30] (to which we refer the reader for further details on the background evolution of these models) it was shown that these choices of parameters are free of ghost and Laplace instabilities (of the scalar fluctuations) for initial conditions with $\rho_{\varphi,i}/\rho_{m,i} \sim 10^{-5}$. Here we shall use this and other choices of initial conditions which have not shown any theoretical instabilities of the scalar perturbations throughout the entire expansion history. In Table 2.2 we list all these initial conditions with the derived values of the c_2 parameter and age of the Universe. In this chapter, it is not our goal to place formal constraints on the parameter space of the model and therefore we shall not be worried about the scaling degeneracy of Eq. (2.65).

Figure 2.1 shows the time evolution of the ratio of the Hubble expansion rates, $H = \theta/3$, of the Galileon and ΛCDM models and of the Galileon field equation-of-state parameter, $w = \bar{p}_\varphi/\bar{\rho}_\varphi$. Figure 2.1 shows that, depending on the initial condition, the expansion rate can be faster or slower than in ΛCDM for different times during the evolution. Another noteworthy aspect of the background evolution is the possibility of having phantom dynamics, $w < -1$ [18, 19, 50]. The initial values of $\rho_{\varphi,i}$ can have a great impact on the evolution of w: the lower $\rho_{\varphi,i}$ the more negative the values of w tend to be at late times. The reason is that lower values of ρ_φ in the past force the energy density of the Galileon field to grow more drastically ($w < -1$) closer to today, in order to become the dominant component to accelerate the expansion [30, 39, 51] (see [48, 49] for expansion history observational constraints). However, for $\rho_{\varphi,i} \lesssim 10^{-5}$, the strong dependence of w on the initial conditions does not propagate into the expansion rate which is only sensitive to changes in w for times sufficiently close to today when dark energy is non-negligible. Moreover, the solutions for $\bar{\rho}_{\varphi,i} \lesssim 10^{-5}$

Table 2.1 The model parameters for the Galileon models studied in this chapter

Models	c_3	c_4	c_5	c_G
Galileon 1	12.8	−1.7	1.0	0
Galileon 2	6.239	−2.159	1.0	0
Galileon 3	5.73	−1.2	1.0	0
Galileon 4	5.73	−1.2	1.0	−0.4

The c_2 parameter is tuned to yield the required amount of dark energy today and its exact value depends on the choice of the initial Galileon energy density $\rho_{\varphi,i}$

Table 2.2 The values of the parameter c_2 and of the age of the Universe for all the initial conditions used in this chapter

$\rho_{\varphi,i}/\rho_{m,i}$	c_2	Age (Gyr)
Galileon 1		
10^{-4}	-27.00	13.978
10^{-5}	-27.49	14.317
10^{-6}	-27.56	14.366
10^{-7}	-27.58	14.374
10^{-8}	-27.59	14.375
Galileon 2		
10^{-4}	-12.600	13.614
10^{-5}	-12.846	14.256
5×10^{-6}	-12.857	14.286
10^{-6}	-12.885	14.357
10^{-7}	-12.891	14.372
10^{-8}	-12.892	14.375
Galileon 3		
10^{-4}	-14.760	13.854
10^{-5}	-15.122	14.296
10^{-6}	-15.179	14.363
10^{-7}	-15.188	14.373
10^{-8}	-15.189	14.375
Galileon 4		
10^{-4}	-14.186	13.833
10^{-5}	-14.519	14.285
5×10^{-6}	-14.539	14.312

The age for ΛCDM is 13.738 Gyr

tend to have nearly the same late time evolution of w_φ. This illustrates the different initial condition being attracted to the tracker evolution. In particular, the smaller $\bar{\rho}_{\varphi,i}$ (smaller $\dot{\bar{\varphi}}_i$), the earlier the solutions reach the tracker [39].

2.4.2 Linear Perturbation Results

We now look at the physical predictions of the full linear perturbation equations derived in the previous sections. We always use the best fit parameters from the WMAP 7-year data results [44]: $\Omega_{m0} = 0.265$, $n_s = 0.963$, $H_0 = 100h$ km/s/Mpc ($h = 0.71$), $\Omega_k = 0$, where n_s and Ω_k are the spectral index and the fractional energy density associated with the spatial curvature. Neutrinos are treated as massless in this chapter. These values are obtained for a ΛCDM model and there is no reason to

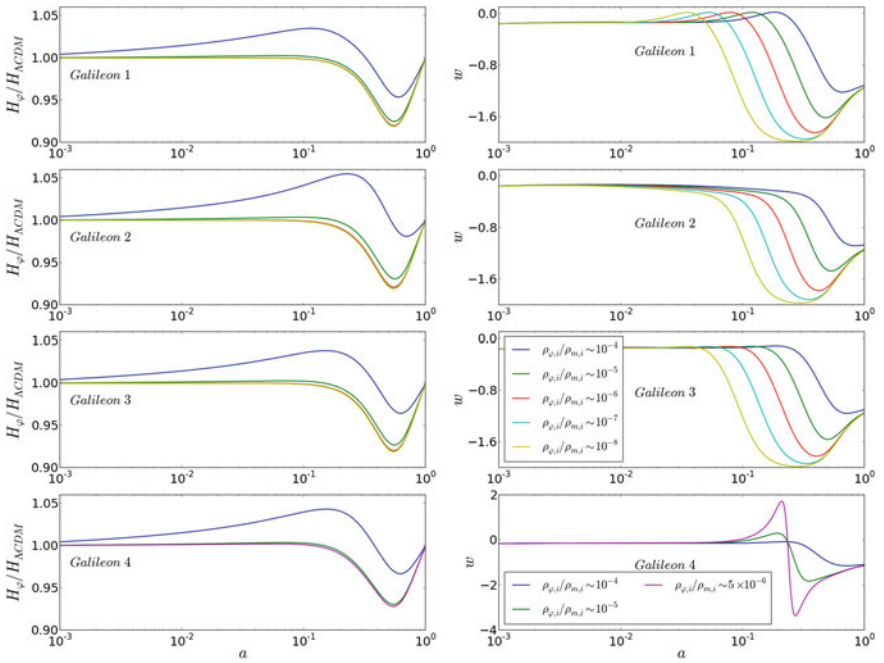


Fig. 2.1 Evolution of the ratio of the Hubble expansion rates of the Galileon and ΛCDM models, $H/H_{\Lambda\mathrm{CDM}}$ ($H = \theta/3$), and of the Galileon field equation of state parameter w. The evolutions are shown for the four models of Table 2.1 for different initial conditions, as labelled. Figure reproduced from Ref. [1]

believe they should be the same in a Galileon cosmology. However, in our analysis here, we prefer to focus only on the differences to ΛCDM driven by the Galileon field *per se*, and not by different cosmological parameters. The determination of the best-fitting cosmological parameters from the CMB obtained assuming Galileon cosmologies is the subject of Chap. 3. The amplitude of the primordial curvature perturbations is $A_s = 2.43 \times 10^{-9}$ at a pivot scale $k_0 = 0.002\mathrm{Mpc}^{-1}$.

As a consistency test of the results that follow, we checked that the perturbed quantities we obtain from `CAMB` satisfy the k-space conservation equations (2.57, 2.58).

CMB

In Fig. 2.2, we plot the CMB power spectrum for the Galileon 3 model and ΛCDM together with the WMAP 7-year [52] (squares) and ACT [53] (circles) data. Figure 2.3 is the same as Fig. 2.2 but for the four models of Table 2.1 with a log-scaled x-axis which highlights the low-l region. The effect of the Galileon field in the CMB power spectrum is mainly two-fold.

Firstly, the modifications of the expansion rate can shift the positions of the CMB acoustic peaks. The value of the initial condition has an impact on the background

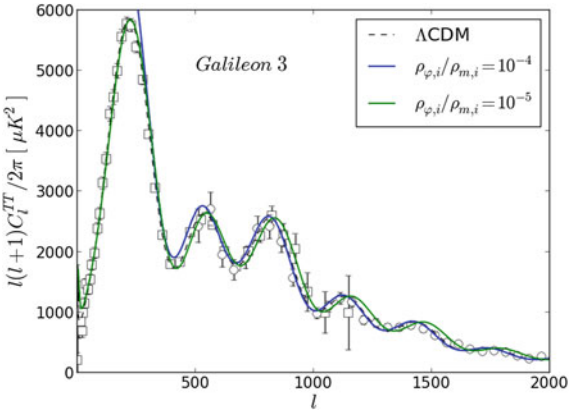


Fig. 2.2 CMB temperature power spectra for the Galileon 3 model with two different initial conditions and for ΛCDM (*dashed black*), together with the WMAP 7-year (*squares*) [52] and ACT (*circles*) [53] data. Figure reproduced from Ref. [1]

expansion rate and hence on the distance to the surface of last scattering, which translates into different positions for the peaks. For sufficiently small values of $\rho_{\varphi,i}/\rho_{m,i} \lesssim 10^{-5}$ (not plotted in Fig. 2.2 since they are indistinguishable from the $\rho_{\varphi,i}/\rho_{m,i} = 10^{-5}$ case) the Galileon 3 curves have essentially the same peaks positions since the expansion rate becomes insensitive to $\rho_{\varphi,i}/\rho_{m,i}$ (cf. Fig. 2.1). The same applies for the Galileon 1, Galileon 2 and Galileon 4 models.

Secondly, the late time evolution of the gravitational potential can be also different from ΛCDM, resulting in a modified signal of the ISW effect on the largest angular scales (low l in Fig. 2.3). For instance, the choice $\rho_{\varphi,i}/\rho_{m,i} = 10^{-4}$ is completely ruled out for all the models shown, since the spectrum at low l is larger than the observational data by several orders of magnitude. In this case, the ISW effect is so pronounced that it dominates over the first acoustic peak and can also have an impact on the second and third ones.

Lowering the initial amount of dark energy helps to reconcile the models with the data. However, for Galileon 4 there is still too much power on large scales. Note that this model differs from Galileon 3 by having a non-vanishing value of c_G and it is impossible to keep lowering the initial Galileon density ($\rho_{\varphi,i}/\rho_{m,i} \sim 5 \times 10^{-6}$) as Laplace instabilities start to appear. This hints that the strength of the derivative coupling c_G can have a crucial impact on the predictions. For all the other models (Galileon 1 to Galileon 3), for sufficiently small values of $\rho_{\varphi,i}/\rho_{m,i}$, the dependence on the initial conditions becomes less pronounced and the fit to the CMB improves. There are still differences from the best fit ΛCDM model and from the data at low l, but since the errorbars are also larger due to cosmic variance, Galileon 1 to Galileon 3 models may still be compatible with the observations.

It is interesting to note that the CMB power spectrum for the Galileon 1 and Galileon 3 models can be quite similar although their c_3 and c_4 parameters are different. This shows that there are, to some extent, degeneracies in the Galileon model parameter space. On the other hand, changing only one of the Galileon parameters can also change considerably the CMB predictions. For instance, in the top-right

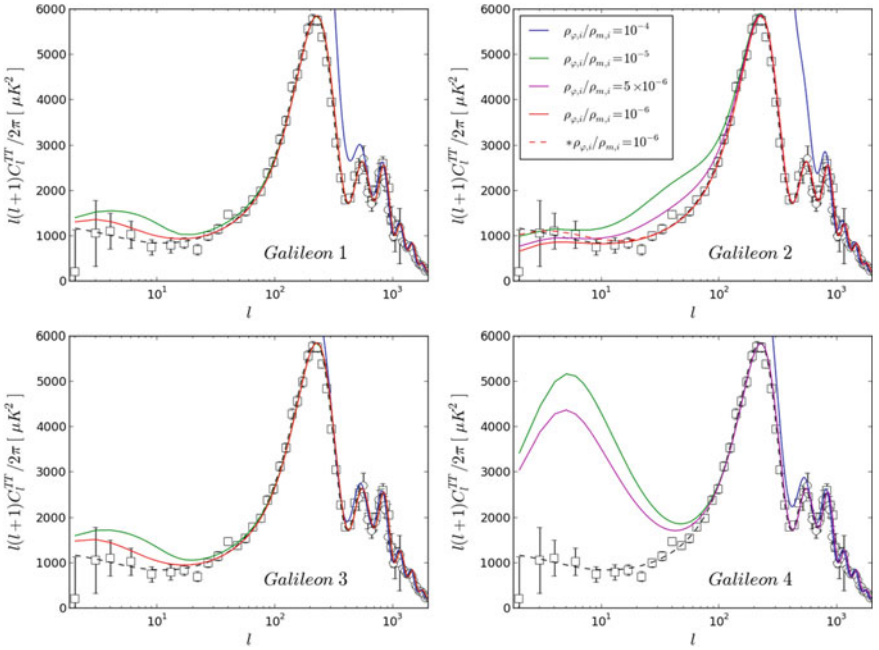


Fig. 2.3 CMB power spectra for the four Galileon models for different initial conditions and ΛCDM, together with the WMAP 7-year data (*squares*) [52] and ACT (*circles*) [53] data. Figure reproduced from Ref. [1]

panel we plot the CMB power spectrum of a model sharing all the parameters of Galileon 2 in Table 2.1 except that $c_4 = -1.659$, for $\rho_{\varphi,i}/\rho_{m,i} = 10^{-6}$ (dashed red). Note that c_2 also differs because it is tuned to yield the required amount of dark energy today, giving $c_2 = -14.968$. We see that by changing only c_4 the predicted CMB spectrum gets closer to the data for the lowest values of l. It is also interesting to note that all the models have the value of c_5 fixed and we expect a richer phenomenology if we allow this parameter to vary as well.

To further understand the CMB predictions of the Galileon model at low l, we plot in Fig. 2.4 the time evolution of the Weyl potential, ϕ, which is the relevant quantity for the ISW effect. We show the evolution for different values of k for the initial condition $\rho_{\varphi,i}/\rho_{m,i} = 10^{-5}$. The variety of evolutions can be very rich within the parameter space of the Galileon model and depends on the scale under consideration. The evolution of ϕ agrees, to some extent, with the ΛCDM model during the radiation dominated era. However, in the matter era, while ϕ is constant in the ΛCDM model, that is not the case for Galileon gravity and the gravitational potential does evolve with time. In particular, we note a very pronounced variation with time of ϕ for Galileon 4 during the matter era and today which explains why there is so much power at low l in this model (c.f. Fig. 2.3). Moreover, for the models shown, the gravitational potential suffers an overall deepening with time [30, 51, 54, 55], in clear contrast with the ΛCDM model where the gravitational potential gets

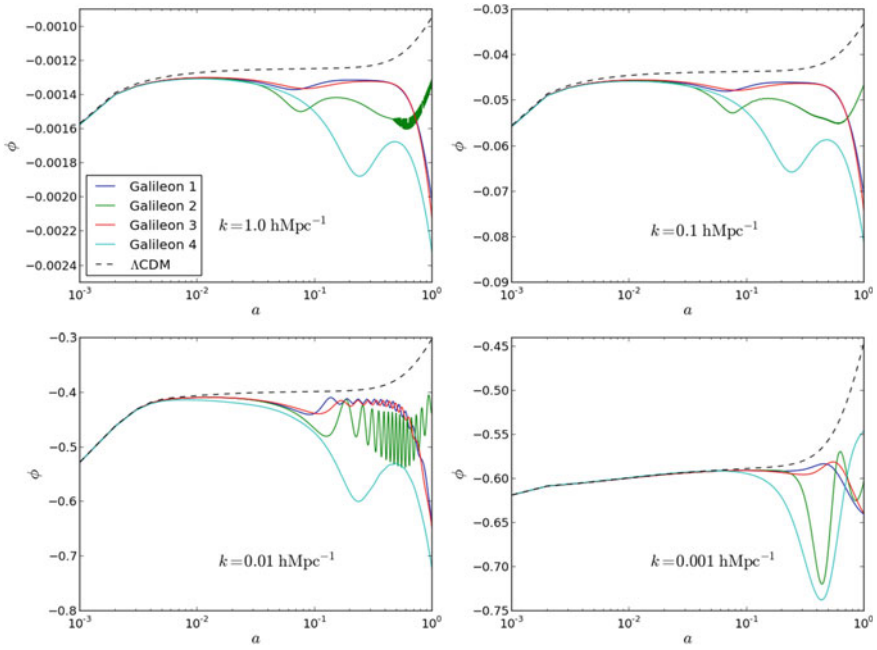


Fig. 2.4 Time evolution of the Weyl (lensing) gravitational potential ϕ for the four Galileon models and ΛCDM (*dashed*) for $k = \{1.0,\ 0.1,\ 0.01$ and $0.001\}$ hMpc^{-1}. All the models have the initial condition $\rho_{\varphi,i}/\rho_{m,i} = 10^{-5}$. Figure reproduced from Ref. [1]

shallower with the onset of the accelerated expansion. We shall analyse this feature with more detail in Sect. 3.3.2, but we anticipate here that the late-time deepening of the lensing potential has a very strong potential to rule out the entire Galileon model!

Weak Lensing Power Spectrum

The weak lensing signal of the CMB anisotropies is determined by the projected lensing potential ψ, which is an effective potential obtained by integrating the Weyl potential, ϕ, from today to the time of last scattering [56] (see also [57] for a concise description and application to modified gravity theories).

The angular power spectrum of ψ is plotted in Fig. 2.5 for the four Galileon models and we see that it can be noticeably larger than the ΛCDM result on all scales, which follows from the larger values (in magnitude) of ϕ in these models (cf. Fig. 2.4). The Galileon 4 model is the one where the gravitational potential deepens the most with time and it is therefore the model with the most lensing power. The initial conditions also have an impact on the result, especially for $\rho_{\varphi,i}/\rho_{m,i} \gtrsim 10^{-6}$. For instance, for the case $\rho_{\varphi,i}/\rho_{m,i} = 10^{-4}$ (which is not plotted) the power is higher by several orders of magnitude for all the models.

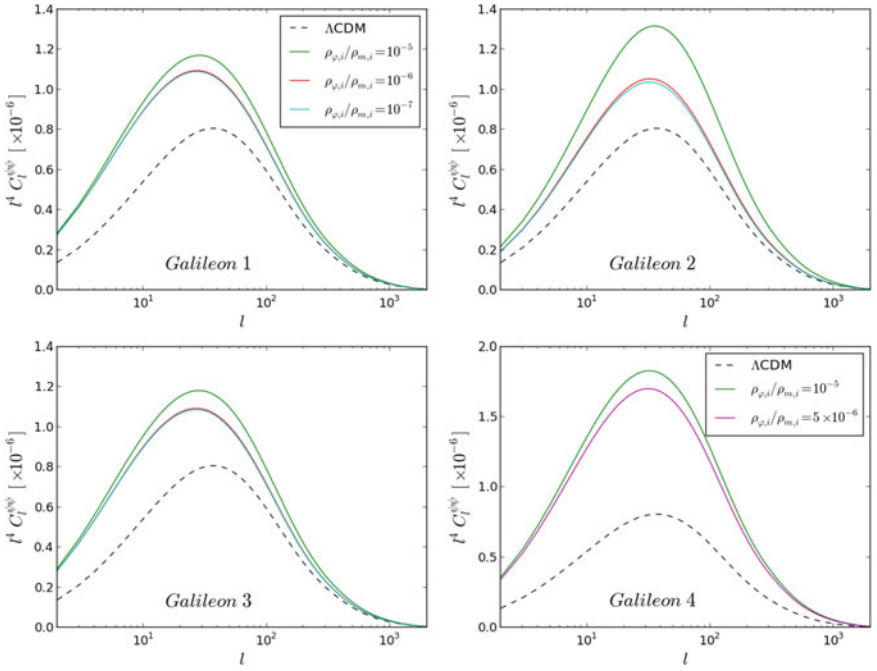


Fig. 2.5 Angular power spectrum of the weak lensing potential ψ for the four Galileon models with different initial conditions and ΛCDM (*dashed*). Figure reproduced from Ref. [1]

This is an important result and it shows that weak lensing measurements have the capability to place strong constraints on the Galileon gravity model. In particular, the Galileon 1 to Galileon 3 models, which have CMB temperature power spectrum predictions similar to that of ΛCDM for $\rho_{\varphi,i}/\rho_{m,i} = 10^{-6}$ (red line), nevertheless have very distinctive predictions for the power spectrum of the lensing potential. In Chap. 3, measurements of $C_l^{\psi\psi}$ shall be used to constrain the model.

Matter Power Spectrum

Figure 2.6 shows the linear matter power spectrum predicted in the different models. We have chosen to plot the power spectra at redshift $\bar{z}_{LRG} = 0.31$, which is the median redshift of luminous red galaxies (LRGs) in DR7 from the Sloan Digital Sky Survey (SDDS) [60]. A recent estimate of the power spectrum of LRGs is shown by the points with errorbars reproduced in each panel [58]. By plotting the matter power spectrum at the same redshift as the measurement, there is no need to make any adjustment for the growth factor to compare theory to observation. However, since we are plotting the prediction of linear perturbation theory in real space, there are three effects which could be responsible for any discrepancies between the theoretical spectra and the measurement: (1) Galaxy bias. This is generally modelled as a constant shift in the amplitude of the power spectrum on large scales, though simulations show that the

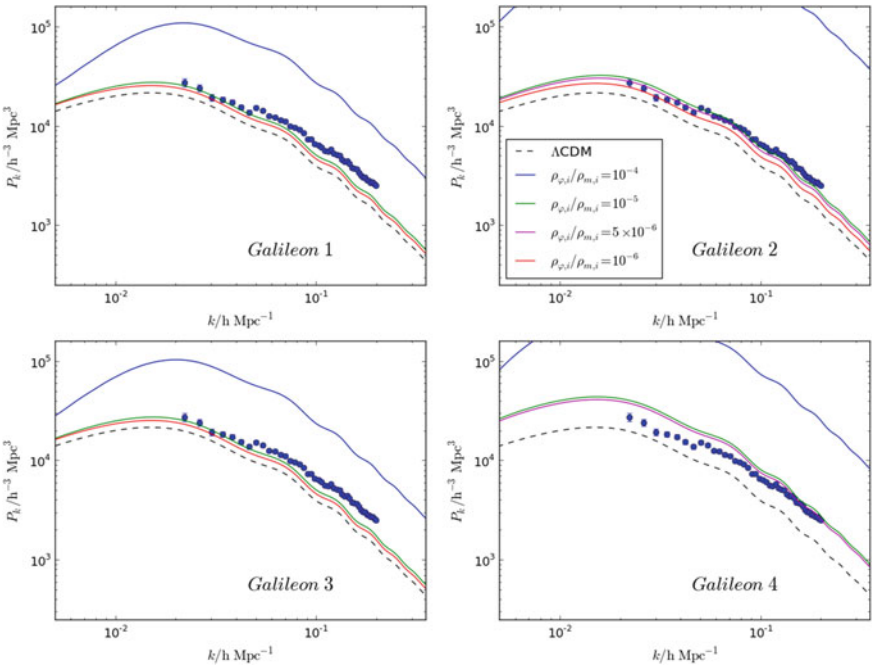


Fig. 2.6 Matter power spectrum at redshift $\bar{z}_{LRG} = 0.31$ for the four Galileon models with different initial conditions and ΛCDM (*dashed*), together with the SDSS-DR7 LRG host halo power spectrum [58]. The measurements are scaled by a factor of 1.85^{-2} [59] and $\bar{z}_{LRG}$ is the mean redshift of the LRG sample. Figure reproduced from Ref. [1]

bias is scale dependent, particularly for highly clustered objects [61]. (2) Redshift-space distortions. Using peculiar velocities to infer the radial distance to a galaxy introduces a systematic shift in the clustering amplitude. Again, this can be scale dependent [62]. (3) Non-linear effects. This includes the familiar mode coupling between fluctuations on different scales, but also, in the case of the Galileon models, possible screening effects which could introduce scale dependent departures from the linear perturbation theory predictions. It is important to note also that the amplitude of the actual LRG power spectrum shown in Fig. 2.6 is scaled down by a factor of 1.85^{-2}, as explained in the Erratum [59].

A robust comparison between theory and observations should take all three complications above into account. This shall be done in Chap. 5 using Halo Occupation Distribution (HOD) methods applied on the results from N-body simulations. For now, we simply note that the difference to ΛCDM depends sensitively on the value of $\rho_{\varphi,i}/\rho_{m,i}$. For instance, the initial condition $\rho_{\varphi,i}/\rho_{m,i} = 10^{-4}$ has a substantial excess of power relative to ΛCDM, which suggests it may be hard to reconcile these models with the data. Lowering $\rho_{\varphi,i}/\rho_{m,i}$ brings the Galileon models into closer agreement with ΛCDM and the results become less sensitive to the initial conditions (lower initial conditions have nearly the same prediction as $\rho_{\varphi,i}/\rho_{m,i} = 10^{-6}$). However, all

the models still produce an excess of power when compared to ΛCDM indicating that the formation of linear structure is enhanced by the modifications of gravity in the Galileon model, a conclusion in agreement with previous linear perturbation studies in the literature [30, 51, 54, 63]. The Galileon 4 model is the one where the effects are the most pronounced. This indicates, once again, that the c_G parameter can have a critical impact on the results.

Clustering of the Galileon Field

We now turn the attention to the time evolution of the linear density contrast of the Galileon field $\delta_\varphi = \rho_\varphi/\bar{\rho}_\varphi - 1$. This is plotted in Fig. 2.7 for the initial condition $\rho_{\varphi,i}/\rho_{m,i} = 10^{-5}$. We see that the Galileon density contrast (dashed lines) can be large, being comparable with the dark matter (solid lines) and baryonic matter (dotted lines) density contrasts throughout most of the evolution. This happens for all the scales considered including small scales such as $k = 1.0\ \mathrm{hMpc}^{-1}$.

This strong clustering of the Galileon field has a large impact on the evolution of the Weyl gravitational potential ϕ which directly determines many observables such as the ISW effect (cf. Fig. 2.3), weak lensing (cf. Fig. 2.5) and clustering of matter (cf. Fig. 2.6).

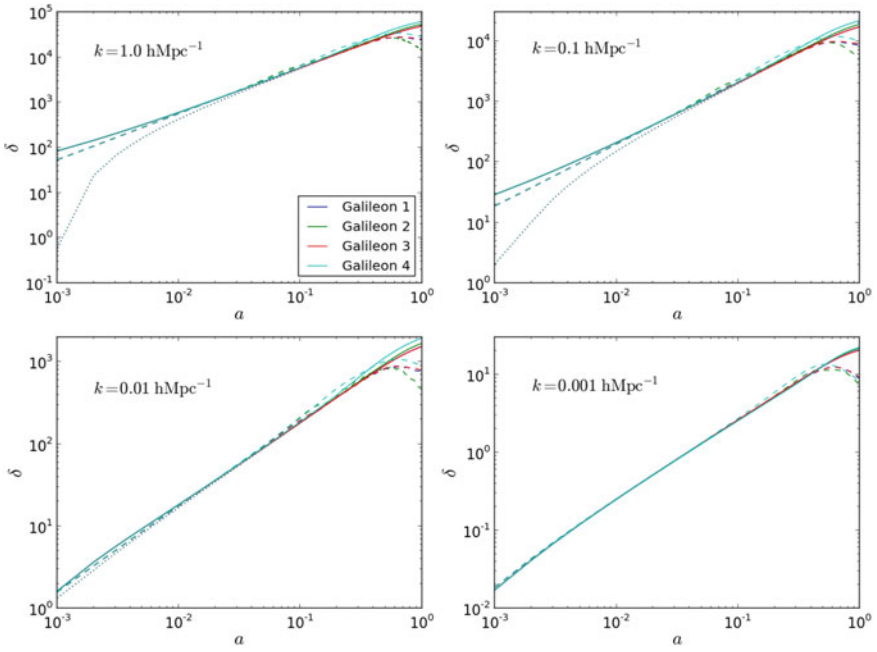


Fig. 2.7 Time evolution of the linear density contrast of dark matter (DM, *solid lines*), $\delta_{\mathrm{DM}} = \rho_{DM}/\bar{\rho}_{DM} - 1$, baryonic matter (B, *dotted lines*), $\delta_{\mathrm{B}} = \rho_B/\bar{\rho}_B - 1$, and Galileon field (*dashed lines*), $\delta_\varphi = \rho_\varphi/\bar{\rho}_\varphi - 1$, for the four Galileon models for $k = \{1.0,\ 0.1,\ 0.01$ and $0.001\}\ \mathrm{hMpc}^{-1}$. All the models have initial condition $\rho_{\varphi,i}/\rho_{m,i} = 10^{-5}$. Figure reproduced from Ref. [1]

Quasi-static Limit Approximation

In Fig. 2.8 we plot the time evolution of the k-space Galileon perturbation, γ (dashed), along with the corresponding solution obtained in the quasi-static limit (solid). The quasi-static limit is the limit in which the spatial derivatives of the field are dominant over the time derivative ones. Practically, this means neglecting all terms in the field equations that are suppressed by $\mathcal{H}^2/k^2$ or φ'/k^2.

As for the evolution of the density contrast δ_φ and the Weyl potential ϕ, here there is also a strong scale dependence. Moreover, we see that even for near-horizon scales such as $k = 0.001$ hMpc^{-1} the quasi-static limit can be a good (though not perfect) approximation to the full solution. In particular, in the Galileon 2 curves with $k = 0.01$ hMpc^{-1}, one can see that the quasi-static approximation agrees quite well with the full solution despite the oscillations in the latter. The quasi-static limit appears therefore to be valid for many cases in the Galileon model, especially when one is interested in subhorizon scales.

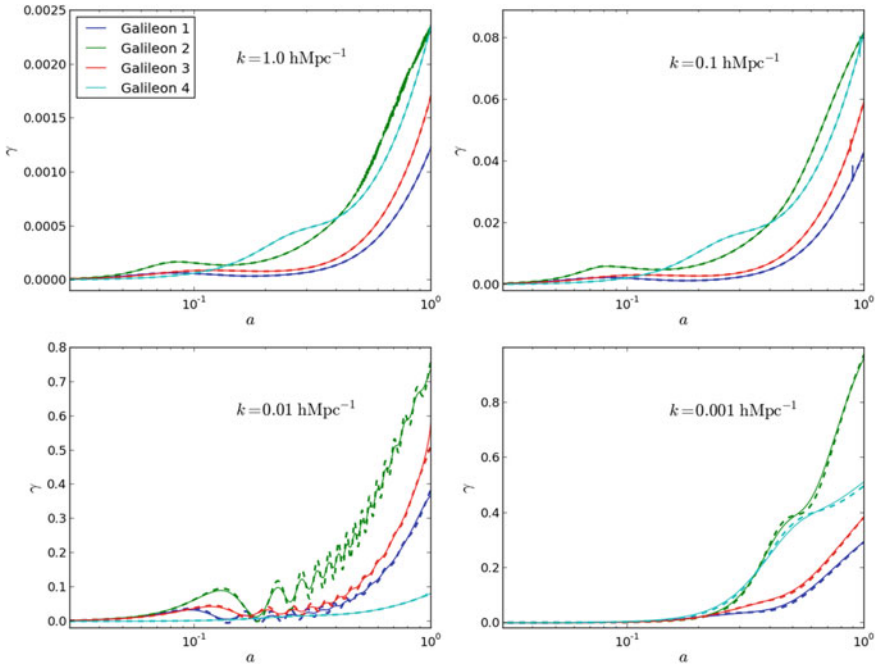


Fig. 2.8 Time evolution of the k-space Galileon field perturbation γ (*dashed*) along with the corresponding quasi-static limit (*solid*), for the four Galileon models for $k = \{1.0,\ 0.1,\ 0.01$ and $0.001\}$ hMpc^{-1}. All the models have initial condition $\rho_{\varphi,i}/\rho_{m,i} = 10^{-5}$.. Figure reproduced from Ref. [1]

2.5 Summary

In this chapter, we took the first step towards constraining Galileon gravity with linear perturbation theory by studying its cosmological preditions for a fixed number of parameter set values. For this, we derived the full CGI perturbation equations, which were then solved using a modified version of the CAMB code. We validated our CAMB code by performing several successful consistency tests.

The main results in this chapter can be summarized as follows:

- The expansion rate in Galileon cosmologies can depend sensitively on the initial value of the Galileon field energy density, especially if the latter is not small, e.g., if $\rho_{\varphi,i}/\rho_{m,i} \gtrsim 10^{-5}$ ($z_i = 10^6$). Throughout the evolution (cf. Fig. 2.1), the expansion rate can be faster or slower than in ΛCDM and the Galileon equation-of-state parameter is phantom-like ($w < -1$) at late times.
- The modified background expansion leads to a visible shift in the positions of the acoustic peaks of the CMB temperature power spectrum. The strongest effect of the Galileon field on the CMB temperature power spectrum, however, appears to be on the largest angular scales (low values of l, cf. Fig. 2.3), where the full power receives a significant contribution from the integrated Sachs-Wolfe effect. This is due to the late-time evolution of the gravitational potential ϕ, which in Galileon models tends to become deeper at late times (more negative), and does so rather rapidly, compared to ΛCDM (cf. Fig. 2.4).
- The evolution of the gravitational potential influences a number of cosmological observables, both directly and indirectly. In addition to the ISW effect, it also has a strong impact on the growth of matter density perturbations (cf. Fig. 2.6) and gravitational lensing. In particular, we have shown that the Galileon model can predict considerably more power than ΛCDM for the weak lensing power spectrum (cf. Fig. 2.5), even if the predictions of the two models for the CMB power spectrum more or less agree. In Chap. 3, we shall use the weak lensing power spectrum data from the Planck mission to constrain the Galileon model.
- We have seen that the Galileon field can cluster substantially (cf. Fig. 2.7) and that the quasi-static approximation for the evolution of the Galileon field perturbation serves as a good approximation on subhorizon scales (cf. Fig. 2.8).
- At first sight, the physics of the Galileon field appears to be described by the nine extra parameters: $\{c_1, c_2, c_3, c_4, c_5, \bar{\varphi}_i, \dot{\bar{\varphi}}_i, \delta\varphi_i, \dot{\delta\varphi}_i\}$. However, $\bar{\varphi}_i$, is an irrelevant parameter since it never enter the equations of the model. Furthermore, the initial values of the field perturbation and its time derivative can be fixed to zero $\delta\varphi_i = \dot{\delta\varphi}_i = 0$, with no impact on the results. In this chapter (and in fact in all this thesis) we always consider $c_1 = 0$, as this is a potential term and we are interested only in cases where the acceleration is driven by kinetic terms. By assuming that (i) the background is spatially flat and (ii) that the field evolves according to the tracker solution, then two of the Galileon parameters are given in terms of the others (cf. Sect. 2.3). Finally, the need to break the scaling degeneracy of the model, allows one to fix one more parameter (cf. Sect. 2.3). If all these considerations are

applied, then the Galileon model that we shall study in the remainder of this thesis contains only two extra parameters, relative to ΛCDM.

In conclusion, we have shown that the detailed study of the full perturbation equations unveils a rich phenomenology in Galileon gravity models. The results presented in this chapter also show that the model predictions depend sensitively on the exact parameter combinations. The indications are that strong constraints can be placed on the parameter space of the model, which is precisely what we shall determine in the next chapter.

References

1. Barreira A, Li B, Baugh CM, Pascoli S (2012) Linear perturbations in Galileon gravity models. Phys Rev D86:124016. arXiv:1208.0600
2. Nicolis A, Rattazzi R, Trincherini E (2009) Galileon as a local modification of gravity. Phys Rev D 79:064036
3. Deffayet C, Esposito-Farèse G, Vikman A (2009) Covariant galileon. Phys Rev D 79:084003
4. Dvali G, Gabadadze G, Porrati M (2000) 4D gravity on a brane in 5D Minkowski space. Phys Lett B 485:208–214 arXiv:hep-th/0005016
5. Luty MA, Porrati M, Rattazzi R (2003) Strong interactions and stability in the DGP model. JHEP 9:29 arXiv:hep-th/0303116
6. Nicolis A, Rattazzi R (2004) Classical and quantum consistency of the DGP model. JHEP 6:59 arXiv:hep-th/0404159
7. Luty MA, Porrati M, Rattazzi R (2003) Strong interactions and stability in the dgp model. JHEP 2003(09):029
8. Nicolis A, Rattazzi R (2004) Classical and quantum consistency of the dgp model. JHEP 2004(06):059
9. Gorbunov D, Koyama K, Sibiryakov S (2006) More on ghosts in the dvali-gabadaze-porrati model. Phys Rev D 73:044016
10. Gregory R, Kaloper, Myers RC, Padilla A (2007) A new perspective on DGP gravity. JHEP 0710:069. arXiv:0707.2666
11. Woodard RP (2007) Avoiding dark energy with 1/r modifications of gravity. Lect Notes Phys 720:403–433. arXiv:astro-ph/0601672
12. Hinterbichler K, Trodden M, Wesley D (2010) Multi-field galileons and higher co-dimension branes. Phys Rev D 82:124018. arXiv:1008.1305
13. Deffayet C, Deser S, Esposito-Farese G (2009) Generalized Galileons: all scalar models whose curved background extensions maintain second-order field equations and stress-tensors. Phys Rev D 80:064015. arXiv:0906.1967
14. Gleyzes J, Langlois D, Piazza F, Vernizzi F (2014) Healthy theories beyond Horndeski. arXiv:1404.6495
15. Horndeski GW (1974) Second-order scalar-tensor field equations in a four-dimensional space. Int J Theor Phys 10:363–384
16. Deffayet C, Gao X, Steer DA, Zahariade G (2011) From k-essence to generalised Galileons. Phys Rev D 84:064039. arXiv:1103.3260
17. Kobayashi T, Yamaguchi M, Yokoyama J (2011) Generalized G-inflation: inflation with the most general second-order field equations. Prog Theor Phys 126:511–529. arXiv:1105.5723
18. Deffayet C, Pujolas O, Sawicki I, Vikman A (2010) Imperfect dark energy from kinetic gravity braiding. JCAP 1010:026. arXiv:1008.0048
19. Pujolas O, Sawicki I, Vikman A (2011) The imperfect fluid behind kinetic gravity braiding. JHEP 1111:156. arXiv:1103.5360

20. Kimura R, Kobayashi T, Yamamoto K (2012) Observational constraints on kinetic gravity braiding from the integrated sachs-wolfe effect. Phys Rev D 85:123503. arXiv:1110.3598
21. Charmousis C, Copeland EJ, Padilla A, Saffin PM (2012) General second order scalar-tensor theory, self tuning, and the fab four. Phys Rev Lett. 108:051101. arXiv:1106.2000
22. Charmousis C, Copeland EJ, Padilla A, Saffin PM (2012) Self-tuning and the derivation of a class of scalar-tensor theories. Phys Rev D 85:104040. arXiv:1112.4866
23. Bruneton J-P, Rinaldi M, Kanfon A, Hees A, Schlogel S et al. (2012) Fab Four: When John and George play gravitation and cosmology. 1203:4446
24. Copeland EJ, Padilla A, Saffin PM (2012) The cosmology of the Fab-Four 1208:3373
25. Appleby SA, De Felice A, Linder EV (2012) Fab 5: noncanonical kinetic gravity, self tuning, and cosmic acceleration. JCAP 1210:060. arXiv:1208.4163
26. Kobayashi T, Tashiro H, Suzuki D (2010) Evolution of linear cosmological perturbations and its observational implications in Galileon-type modified gravity. Phys Rev D 81:063513. arXiv:0912.4641
27. Kobayashi T (2010) Cosmic expansion and growth histories in Galileon scalar-tensor models of dark energy. Phys Rev D 81:103533. arXiv:1003.3281
28. Leon G, Saridakis EN (2012) Dynamical analysis of generalized Galileon cosmology. 1211:3088
29. Burrage C, Kaloper N, Padilla A (2012) Strong coupling and bounds on the graviton mass in massive gravity. 1211:6001
30. Appleby SA, Linder EV (2012) The paths of gravity in Galileon cosmology. JCAP 1203:043. arXiv:1112.1981
31. Sushkov SV (2009) Exact cosmological solutions with nonminimal derivative coupling. Phys Rev D 80:103505. arXiv:0910.0980
32. Gubitosi G, Linder EV (2011) Purely kinetic coupled gravity. Phys Lett B 703:113–118. arXiv:1106.2815
33. de Rham C, Heisenberg L (2011) Cosmology of the Galileon from massive gravity. Phys Rev D 84:043503. arXiv:1106.3312
34. Van Acoleyen K, Van Doorsselaere, J (2011) Galileons from Lovelock actions. Phys Rev D 83:084025. arXiv:1102.0487
35. Zumalacarregui M, Koivisto TS, Mota DF (2012) DBI Galileons in the Einstein Frame: Local Gravity and Cosmology. arXiv:1210.8016
36. Amendola L (1993) Cosmology with nonminimal derivative couplings. Phys.Lett B 301:175–182. arXiv:gr-qc/9302010
37. Challinor A, Lasenby A (1999) Cosmic microwave background anisotropies in the CDM model: a covariant and gauge invariant approach. Astrophys J 513:1–22. arXiv:astro-ph/9804301
38. Ma C-P, Bertschinger E (1994) Cosmological perturbation theory in the synchronous versus conformal Newtonian gauge. Astrophys J arXiv:astro-ph/9401007
39. De Felice A, Tsujikawa S (2010) Cosmology of a covariant Galileon field. Phys Rev Lett 105:111301. arXiv:1007.2700
40. De Felice A, Tsujikawa S (2011) Generalized Galileon cosmology. Phys Rev D 84:124029. arXiv:1008.4236
41. De Felice A, Tsujikawa S (2012) Conditions for the cosmological viability of the most general scalar-tensor theories and their applications to extended Galileon dark energy models. JCAP 1202:007. arXiv:1110.3878
42. Babichev E, Mukhanov V, Vikman A (2008) K-Essence, superluminal propagation, causality and emergent geometry. JHEP 0802:101. arXiv:0708.0561
43. Lewis A. http://camb.info/
44. Larson D, Dunkley J, Hinshaw G, Komatsu, E, Nolta MR et al. (2011) Seven-year wilkinson microwave anisotropy probe (WMAP) observations: power spectra and WMAP-derived parameters. Astrophys J Suppl 192:16. arXiv:1001.4635
45. Sánchez AG, Crocce M, Cabré A, Baugh CM, Gaztañaga E (2009) Cosmological parameter constraints from SDSS luminous red galaxies: a new treatment of large-scale clustering. MNRAS 400:1643–1664. arXiv:0901.2570

46. Gannouji R, Sami M (2010) Galileon gravity and its relevance to late time cosmic acceleration. Phys Rev D 82:024011. arXiv:1004.2808
47. Chow N, Khoury J (2009) Galileon cosmology. Phys Rev D 80:024037
48. Nesseris S, De Felice A, Tsujikawa S (2010) Observational constraints on Galileon cosmology. Phys Rev D 82:124054. arXiv:1010.0407
49. Amna A, Gannouji R, Sami M (2010) Modified gravity à la galileon: late time cosmic acceleration and observational constraints. Phys Rev D 82:103015
50. Sawicki I, Saltas ID, Amendola L, Kunz M (2012) Consistent perturbations in an imperfect fluid. 1208:4855
51. Appleby SA, Linder EV (2012) Galileons on. Trial. 1204:4314
52. Komatsu E et al (2011) Seven-year Wilkinson microwave anisotropy probe (WMAP) observations: cosmological interpretation. Astrophys J Supp 192:18
53. Dunkley J, Hlozek R, Sievers J, Acquaviva V, Ade PAR et al. (2011) Cosmology the atacama, telescope: cosmological parameters from the 2008 power spectra. Astrophys J 739(52). arXiv:1009.0866
54. De Felice A, Kase R, Tsujikawa S (2011) Matter perturbations in Galileon cosmology. Phys Rev D 83:043515. arXiv:1011.6132
55. De Felice A, Kobayashi T, Tsujikawa S (2011) Effective gravitational couplings for cosmological perturbations in the most general scalar-tensor theories with second-order field equations. Phys Lett B 706:123–133. arXiv:1108.4242
56. Lewis A, Challinor A (2006) Weak gravitational lensing of the cmb. Phys Rept 429:1–65. arXiv:astro-ph/0601594
57. Zhao G-B, Pogosian L, Silvestri A, Zylberberg J (2009) Searching for modified growth patterns with tomographic surveys. Phys Rev D 79:083513. arXiv:0809.3791
58. Reid BA et al. (2010) Cosmological constraints from the clustering of the sloan digital sky survey DR7 luminous red galaxies. Mon Not Roy Astron Soc 404:60–85. arXiv:0907.1659
59. Reid BA et al (2011) Erratum: cosmological constraints from the clustering of the sloan digital sky survey dr7 luminous red galaxies. Monthly Notices R. Astron. Soc. 417(4):3103–3104
60. Eisenstein DJ, Annis J, Gunn JE, Szalay AS, Connolly AJ, Nichol RC, Bahcall NA, Bernardi M et al (2001) Spectroscopic Target Selection for the Sloan Digital Sky Survey: The Luminous Red Galaxy Sample. Ap J 122:2267–2280 arXiv:astro-ph/0108153
61. Angulo RE, Baugh CM, Frenk CS, Lacey CG (2008) The detectability of baryonic acoustic oscillations in future galaxy surveys. MNRAS 383:755–776 arXiv:astro-ph/0702543
62. Jennings E, Baugh CM, Pascoli S (2011) Modelling redshift space distortions in hierarchical cosmologies. MNRAS 410:2081–2094. arXiv:1003.4282
63. Okada H, Totani T, Tsujikawa S (2012) Constraints on f(R) theory and Galileons from the latest data of galaxy redshift surveys. arXiv:1208.4681

http://www.springer.com/978-3-319-33695-4

Structure Formation in Modified Gravity Cosmologies

Barreira, A.

2016, XVIII, 218 p. 59 illus. in color., Hardcover
ISBN: 978-3-319-33695-4